

Received February 2, 2021, accepted February 15, 2021, date of publication February 23, 2021, date of current version March 10, 2021.

Digital Object Identifier 10.1109/ACCESS.2021.3061451

A Review on Glaucoma Disease Detection Using Computerized Techniques

FAIZAN ABDULLAH¹, RAKHSHANDA IMTIAZ², HUSSAIN AHMAD MADNI^{ID 2}, HAROON AHMED KHAN^{ID 2}, (Member, IEEE), TARIQ M. KHAN^{ID 1}, (Member, IEEE), MOHAMMAD A. U. KHAN³, AND SYED SAUD NAQVI^{ID 2}, (Member, IEEE)

¹School of Information Technology, Faculty of Science Engineering and Built Environment, Deakin University, Burwood, VIC 3125, Australia

²Department of Electrical and Computer Engineering, COMSATS University Islamabad, Islamabad 45550, Pakistan

³Department of Electrical Engineering, Namal Institute Mianwali, Mianwali 42200, Pakistan

Corresponding author: Haroon Ahmed Khan (haroon.ahmed@gmail.com)

ABSTRACT Glaucoma is an incurable eye disease that leads to slow progressive degeneration of the retina. It cannot be fully cured, however, its progression can be controlled in case of early diagnosis. Unfortunately, due to the absence of clear symptoms during the early stages, early diagnosis are rare. Glaucoma must be detected at early stages since late diagnosis can lead to permanent vision loss. Glaucoma affects the retina by damaging the Optic Nerve Head (ONH). Its diagnosis is dependent on the measurements of Optic Cup (OC) and Optic Disc (OD) in the retina. Computer vision techniques have been shown to diagnose glaucoma effectively and correctly with little overhead. These techniques measure OC and OC dimensions using machine learning based classification and segmentation algorithms. This article aims to provide a comprehensive overview of various existing techniques that use machine learning to detect and diagnose glaucoma based on fundus images. Readers would be able to understand the challenges glaucoma presents from an image processing and machine learning stand-point and will be able to identify gaps in current research.

INDEX TERMS Glaucoma, convolutional neural networks (CNN), diabetic retinopathy, cup-to-disc ratio (CDR), optic nerve head (ONH), optic cup (OC), optic disc (OD), intra ocular pressure (IOP).

I. INTRODUCTION

Glaucoma is a family of eye diseases that affect the optic nerve. Glaucoma is commonly associated with Intra Ocular Pressure (IOP), but it may also be caused by high blood pressure, migraines, obesity, ethnicity, and family history. High IOP results in damage to the optic nerve [1]–[3]. This phenomenon is prevalent amongst adults and people over 60. The optic nerve deterioration occurs in the region of the Optic Disc (OD) known as Optic Nerve Head (ONH). All forms of Glaucoma are incurable and their damage is mostly irreversible. The only options available to the patients are ways to slow down the rate of progression of this disease. The efficacy of all treatments depend on the early diagnosis of the disease. However, early diagnosis is uncommon due to lack of obvious symptoms. In a study conducted in Japan, it was observed that 93 percent of people affected

by Glaucoma were undiagnosed at the early stages of the disease [4]. Glaucoma can be diagnosed by analyzing fundus images, specifically, by measuring the sizes of OC and OD (a depression in the OD). In a fundus image, OD is oval in shape and yellowish in color. OC is visible as a white color circle inside the OD and enlarges with an increase in the IOP. CDR for the normal eye is 0.65 as given in [6]. Any change in CDR is indicative of the existence of Glaucoma. For a computer to accurately diagnose Glaucoma, it is imperative that it must be able to isolate, detect and segment both the OC and the OD from the retinal image. Analysis of the ratio between the two helps diagnose the occurrence of Glaucoma.

Visual computing systems have been shown to be particularly effective in analyzing medical images and classifying items of interest inside an image. Most visual computing algorithms for medical imaging are fundamentally used to identify shapes and geometries of objects in an image. Visual computing machines need to be trained extensively to identify artefacts of interest in an image. Training such machines to

The associate editor coordinating the review of this manuscript and approving it for publication was Victor Sanchez^{ID}.

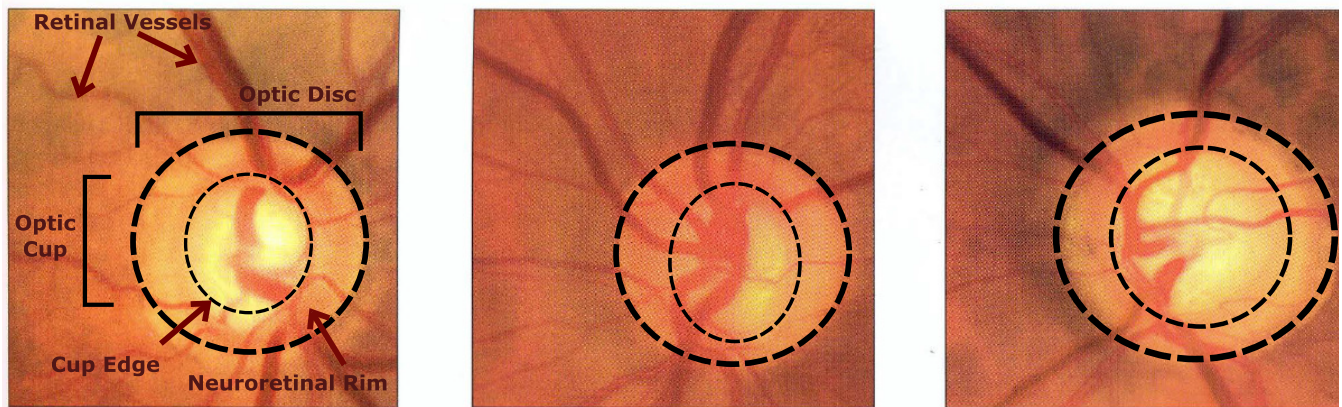


FIGURE 1. The Optic Nerve Head (ONH) in the fundus image. The Optic Disc (OD), Optic Cup (OC) and Neuroretinal Rim have been labelled. The images show a healthy eye, initial state and advanced stage of glaucoma from left to right. The relative expansion of the OC and the thinning of the Neuroretinal Rim is clearly noticeable as is the effect on retinal vessels. Original image courtesy to the Atlas of Clinical Ophthalmology [5].

learn effectively requires a large *dataset*. In context of image analysis, datasets are collections of relevant images where regions of interest have been properly annotated. The number of images may vary from a few hundred to several thousands. It has been shown that the quality of analysis increases substantially with the increase in size of the dataset [7].

Significant work has been done for the automatic analysis of retinal fundus images using computer vision techniques. Machines can be taught to recognize various artefacts in a retinal image like the OC and OD as shown in Figure 1. They can further be trained to measure factors like the CDR. Almazroa *et al.* [8] have been able to train a machine to analyse glaucoma using the publicly available RIGA (Retinal-fundus Images for Glaucoma Analysis) data set with considerable accuracy. Hatanaka *et al.* [9] were able to automatically measure the CDR by performing online profile analysis of retinal images. Artefacts other than OC and OD can be used to detect glaucoma from a retinal image. In the review conducted by Haleem *et al.* [10], various anatomical features to assist early detection of glaucoma have been discussed. These include Vasculature Shift (VS), Peripapillary Atrophy (PPA), Retinal Nerve Fibre Layer (RNFL), and Neuroretinal Rim Notching (NRN) in addition to CDR.

This review aims to provide a detailed analysis of key papers published in this domain to date. A number of different visual computing techniques have been used to detect Glaucoma [11]. In this review, efforts have been made to present a discussion and a multifaceted comparison of these approaches. The techniques reviewed have been segregated in terms of learning approaches (20 of them unsupervised and 22 supervised). For every algorithm, different performance measures for detection of glaucoma have been discussed individually. These measures quantify how well the algorithms detect the disease. These measures include accuracy, sensitivity, specificity and F-scores. At the conclusion of this review, the reader should have a clear understanding of the current state-of-the-art in the use of visual computing systems used to detect glaucoma.

II. DATASETS

Different datasets used in the Glaucoma detection techniques have been described and grouped as follows.

A. SINDI

A study was conducted on Indian population for the analysis of both eyes. People with age range from 40 to 40 to 83 years, were included in the analysis. Previous surgery character was taken into account for the analysis. This dataset contains 5670 normal and 113 Glaucomatous images.

B. SCES

This cross-sectional study took place in Singapore on the basis of population in which 1060 chinese took part. All subjects went through the Optical Coherence Tomography (OCT). This dataset is comprised of 1630 normal images and 46 Glaucomatous images with a sum of 1676 images. This dataset is subjected to classify the images as normal or Glaucomatous.

C. SiMES

For the SiMES, a study was conducted to analyse eye diseases especially in adults living in Malays Singapore. People with age range of 40 to 79 were taken into consideration for the analysis. Patients were assessed by retinal photography, optic disc, ocular biometry and digital lens. The dataset consists of 482 as normal images and 168 as Glaucomatous iamges used for the purpose of classification.

D. ARIA

This dataset is mainly focused on efficient measurement and detection of retinal vessels which can be implemented on both high and low resolution fundus images. This dataset contains 161 images with resolution of 768×576 used for the detection and measurement of retinal vessels and analysis of Glaucoma in the eye.

E. DRISHTI-GS

The Drishti-GS dataset consists of 101 retinal images which are attained from the Aravind eye hospital, India.

The resolution of these retinal image is 2896×1944 where Field of View (FOV) is 30 degree. The age of the patients were in the range of 40 and 80. The groundtruths of OD and OC exist in the dataset. Moreover, the images were annotated by 4 ophthalmologists.

F. RIM-ONE

In RIM-ONE v3, 159 retinal fundus images are present along with their groundtruths that have been annotated by the ophthalmologists. This dataset is comprised of 74 glaucomatous and 85 non glaucomatous images.

G. RIGA

RIGA is a dataset used for the diagnosis of Glaucoma and it stands for Retinal Images for Glaucoma Analysis. This dataset consists of 750 retinal fundus images. These retinal fundus images are acquired from three different resources which are MESSIDOR, Magrabi Eye Centre in Riyadh and Bin Rushed ophthalmic centre in Riyadh. This dataset contains glaucomatous as wells as non-glacomatos images along with their groundtruths that are manually annotated by six ophthalmologists.

H. ORIGA-LIGHT

The retinal fundus images present in the ORIGA-light dataset are collected by the Singapore Malay Eye Study (SiMES) [6]. The process of collection was funded by National Medical Research Council and conducted by the Singapore Eye Research Institute which was completed in the duration of 3 years. This dataset provides the assistance to the researcher for the segmentation of retinal images that helps in the analysis of Glaucoma. This dataset also contains the groundtruths that facilitate the researcher and provides the benchmark for the evaluation of the tools that are designed for the diagnosis of Glaucoma. To study this case, retinal fundus images of both eyes were taken, and the age of the people that were examined, was between 40 and 80. The number images that were kept for making this dataset are 650 in total. Out of 650 images, there are 168 images that are Glaucomatous and other 482 images are nonglaucomatous. This dataset is comprised of retinal fundus images along with their groundtruths. The trained professionals of Singapore Eye Research Institute have segmented and annotated these 650 images that exist in the ORIGA-light dataset.

I. ACRIMA

This dataset consists of 705 retinal images with 396 glaucomatous and 309 healthy images. The retinal images were taken from both eye (i.e. left and right), and were formerly dilated and centred in the OD. The Topcon TRC retinal camera and IMAGEnet capture system were used to capture the retinal images. The FOV of retinal images is 35 degree while resolution is 2048×1536 pixels. The images in this dataset were annotated by two specialists of glaucoma at the Fundación Oftalmológica del Mediterráneo (FOM). To label these images, no other clinical information was used. In the

first version of this dataset, annotations of OD and OC are not given, therefore, it can only be employed for classification purpose.

J. STARE

This dataset is special for Structured Analysis of the Retina (Hoover, Kouznetsova, and Goldbaum 2000). There are 81 retinal images having resolution of 700×605 pixels. The dataset distribution contains 31 normal images and 50 diseased images. This dataset is intended for the segmentation of OD and the blood vessels.

K. ONHSD

It stands for Optic Nerve Head Segmentation dataset (Lowell et al. 2004). It consists of 100 retinal images which were taken from the people belonging to different backgrounds including 20% Asian, 50% Causian, 16% Afro-Caribbean, and 14% patients unknown. The images in this dataset were acquired using Canon CR-6 45MNf. Resolution of retinal images is 640×480 pixels and FOV is 45 degree. The OD is annotated by ophthalmologists and annotations are present in this dataset.

L. DRIVE

This dataset is acquired from the screening program of diabetic retinopathy (DR) in Neitherland and it stands for Digital Retinal Images for Vessel Extraction (Staal et al. 2004). The ages of patients were between 25-90 years. This dataset consists of 40 retinal images which include 33 images having no symptoms of DR and the 7 images having mild symptoms of DR. The Canon CR-5 non-mydiatic 3CCD camera was 768×584 pixels with FOV as 45 degree. In this dataset, FOV of every retinal image is circular, therefore, the diameter of FOV is 540 pixels and a mask image is used to define the FOV. This dataset is distributed into two sets i.e. training and test set, both having equal number of images i.e. 20.

M. DIARETDB1

DIARETDB1 is a public database which contains 89 color images. There are 5 images which are normal and 84 images having at least mild non-proliferative signs (microaneurysms) of the diabetic retinopathy. The camera used to capture these images had 50 degree field-of-view.

N. DRIONS-DB

This dataset consists of 110 images which are manually OD segmented color images. This dataset is special for Digital Retinal Images for the purpose of Optic Nerve Segmentation (Carmona et al. 2008). These images were acquired by two different experts and analogical fundus camera was used to capture the images. HP-photo smart-S20 high resolution scanner was used to digitize these images. It is 8 bits per pixel and has resolution of 600×400 . The average age of patients is 53 years in this dataset having 53.8 percent Caucasian ethnicity female and 46.2 percent Caucasian ethnicity male. The prolonged modest glaucoma was found in 23.1 percent

patients and 76.9 percent had eye hypertension. There were 110 images which had potential issues that can deface the identification procedure of the OD contour.

O. CHASEDB1

This dataset is a reference database of retinal vessels that is obtained from the multiethnic schoolchildren (Owen *et al.* 2011). There are 28 number of retinal images in this dataset in which 20 images are present in test set and remaining 8 images are present in training set (Ng *et al.* 2014). The resolution of these retinal fundus images is 1280×960 pixels and it has FOV of 30 degree. In this dataset, retinal fundus images are categorized on the basis of images with non-uniform background illumination and the images in which blood vessels have poor contrast in comparison with background.

P. REFUGE

There are 1200 retinal images present in this REFUGE dataset. This dataset is categorized into three subdivisions which are training, validation and test. Each category contains equal number of images (i.e. 400 in each). Two different fundus cameras (i.e. Zeiss Visucam 500 and Canon CR-2) were used to capture the retinal fundus images. Zeiss Visucam 500 was used to capture the images for training where Canon-CR-2 was used to acquire the retinal images for validation and test. The resolution for Zeiss Visucam 500 and Canon CR-2 cameras, was 1634×1634 and 2124×2056 pixels respectively. At the posterior pole, all the retinal images are centred with the macula and OD. Images with the glaucoma labels are only present in training datasets which includes 40 glaucomatous and 360 healthy retinal fundus images. The health record was used to acquire the label for training set which shows that it is not acquired on the basis of only retinal fundus images but also using visual field and the OCT. The groundtruths were annotated by 7 ophthalmologists of Zhongshan Ophthalmic center, Sun Yat-sen university, China. The annotations of all 7 ophthalmologists were combined to make the final reference standard.

Q. MESSIDOR

This dataset consists of 1200 retinal fundus images that are attained by 3 departments of ophthalmology. Its name stands for Method to evaluate segmentation and indexing techniques in the field of retinal ophthalmology (Decencière, X. Zhang, *et al.* 2014). Out of 1200 retinal images, there are 800 images that were attained using pupil dilation and other 400 images were attained without pupil dilation. The color video 3CCD camera was used to capture these retinal images on a Topcon TRC NW6 non-mydiatic retinograph. Field of view of these images is 45 degree and having resolution of 1440×960 , 2240×1488 or 2304×1536 pixels. For every retinal image, medical specialists provided retinopathy grade and the risk of macular oedema.

R. HRF

The High- Resolution Fundus (HRF) dataset (Köhler *et al.* 2013) comprises of 45 images. This dataset includes 15 healthy images, 15 glaucomatous images, and 45 retinal images that are affected by diabetic retinopathy. The resolution of these images is 3504×2336 pixels and field of view is 45. These retinal images were taken by the Canon-CR-1 fundus camera.

All datasets are enlisted in Table 1.

III. STRUCTURAL CHANGES DUE TO GLAUCOMA

Glaucoma causes irreparable structural changes in the eye. In this section, we will try to review these structural changes to appreciate all approaches in diagnosing this disease. The structure most affected by Glaucoma is the Optic Nerve Head (ONH). This section describes some of these changes that can be detected visibly in an ophthalmoscope image.

A. OPTIC DISC ASYMMETRY

If the difference of the CDR between both eyes exceeds a certain threshold, it is indicative of Glaucoma [27]. This is especially obvious in the earlier stages of the Glaucoma [28]. As it is the most obvious and persistent symptom across all forms of Glaucoma, it is the single most important visual symptom [29], [30].

B. LOSS OF NEURORETINAL RIM

The neuroretinal rim is the area between the edge of the cup and the disc. In glaucoma, the cup may extend to touch the edge of the disc and may result in the total cupping of the disc and loss of the neuroretinal rim [31]. The thinning of the rim can be used for early diagnosis of glaucoma [32].

C. DISC HEMORRHAGES

Small splinter and flame shaped hemorrhages visible in the retinal layer of the nerve fiber are indicative of some kind of Glaucoma [33]. Hemorrhages typically indicate the presence of either “Normal Tension Glaucoma” [34] or “Primary Open Angle Glaucoma” [35].

D. PERIPAPILLARY ATROPHY (PPA)

Peripapillary Atrophy is a symptom that can be detected visibly. It describes the atrophy of the retinal layers and the retinal pigment epithelium (RPE) around the OD. An association between the progression of peripapillary atrophy has been well established with the progression of glaucoma, where the glaucomatous damage manifests itself in the optic disc resulting in progressive visual field loss [36], even though PPA can occur in healthy subjects as well [37]. PPA is divided into alpha (α) and beta (β) regions [38]. The frequency of β PPA amongst patients of “Open Angle Glaucoma” is shown to be significantly higher than its occurrence in healthy eyes [39] and is detectable using visual computing techniques [40].

TABLE 1. Datasets used for the detection of glaucoma.

Dataset	Source	Availability	Number of Images			Information of Ground Truth
			Normal	Glaucomatous	Total	
SINDI	[12]	Private	5670	113	5783	Glaucomatous and normal class labels for classification
SCES	[13]	Private	1630	46	1676	Glaucomatous and normal class labels for classification
SiMES	[14]	Private	482	168	650	Glaucomatous and normal class labels for classification
ARIA	[15]	Private	101	60	161	Vessel detection, measurement of vessel diameter
DRISHTI-GSI	[16]	Public	31	70	101	Glaucomatous and normal class labels for classification. Segmentation masks of optic nerve head
RIMONE	[17]	Public	92	39	131	Glaucomatous and normal class labels for classification
RIGA	[8]	Public	-	-	750	Segmentation masks of OC and OD
ORIGA	[6]	Public	482	168	650	Glaucomatous and normal class labels for classification. Segmentation masks of OC and OD
ACRIMA	[18]	Public	309	396	705	Glaucomatous and normal class labels for classification
STARE	[19]	Private	31	50	81	Segmentation of OD and blood vessels, Glaucoma classification
ONHSD	[20]	Private	50	50	100	Segmentation of Optic Nerve Head
DRIVE	[21]	Private	33	7	40	Glaucoma classification
DIARETDB1	[22]	Public	5	84	89	Vessel extraction of Digital Retinal Images
DRIONS-DB	[23]	Public	55	55	110	Diabetic retinopathy
CHASEDB1	[24]	Private	-	-	28	OC segmentation. Identification of Optic Nerve Head
REFUGE	[24]	Public	1080	120	1200	Glaucomatous and normal class labels for classification. Annotations of OC and OD (pixel-wise). Masks of Fovea
MESSIDOR	[25]	Public	-	-	1200	Glaucomatous, normal and DR class labels for classification. Automatic Lesion Segmentation
HRF	[26]	Public	15 *DR 15	15	45	Glaucomatous, normal and DR class labels for classification. Glaucomatous, normal and DR class labels for classification. Segmentation masks of blood vessels, OD and FOV

E. VASCULAR CHANGES

A strong association between glaucoma and changes to the retinal vascular structure has been established fairly recently [41]. Narrowing of the retinal vessels is indicative of advanced optic nerve damage due to glaucoma [38]. This is a potential area that can be leveraged to detect glaucoma but is limited due to the fact that baseline values for vascular structure have not been conclusively established yet.

IV. VISUAL SYMPTOMS OF GLAUCOMA IN RETINAL IMAGES

Computerized diagnosis of glaucoma is performed by analyzing retinal images. An understanding of the visual symptoms of glaucoma in these images is fundamental to appreciate the challenges in computerized diagnosis of glaucoma. There are a variety of retinal image acquisition modalities including fundus (ophthalmic) photography, stereo fundus photography, hyperspectral imaging (HSI), fluorescein angiography

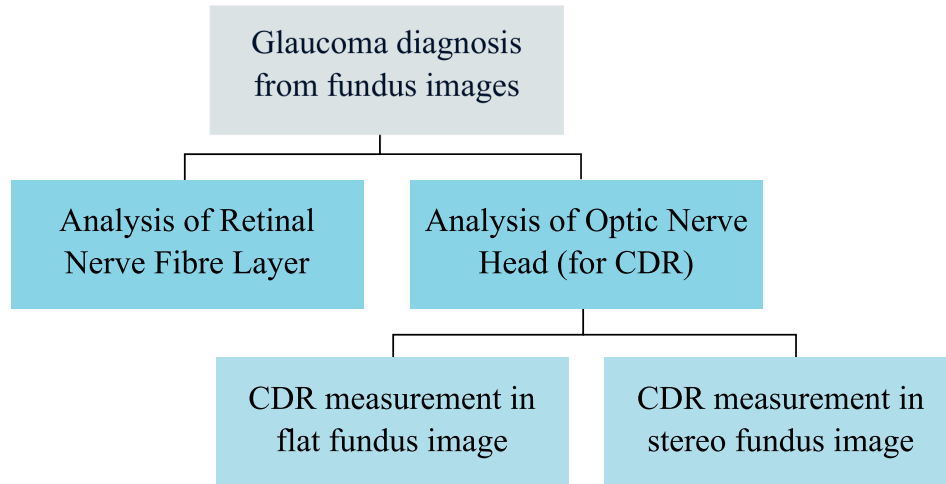


FIGURE 2. Diagnosis of glaucoma in retinal fundus images.

(FA), scanning laser ophthalmoscope (SLO) and optical coherence tomography (OCT) [42]. Any one of these modalities can be used to acquire images from the eye that can be used for the diagnosis of glaucoma using visual computing techniques. However, retinal fundus photographs are most commonly used since they are economical and the screening of diseases using visual computing techniques is quite simple [43]. Ophthalmoscopy, also known as funduscopy, is the process used to acquire the retinal fundus images.

Visual computing algorithms can analyse these images to detect visible symptoms indicating progression of glaucoma. The two main visual symptoms that are most commonly searched for are the defect in the retinal fibre layer and the CDR in the optical nerve head. The use of fundus images for the diagnosis of glaucoma has been summarized in figure 2.

A. ANALYSIS OF THE RETINAL NERVE FIBRE LAYER

The retinal nerve fiber layer defect (NFLDs) is a fundamental sign of Glaucoma that appears as a dark pattern spreading out from the ONH. The nerve fiber layer (NFL) can be observed in fundus photography, OCT and the scanning laser polarimetry. Computerized analysis of NFL in retinal fundus photographs is common. The pattern of NFL has been analyzed and measured by comparing pixel values around and inside the NFL [44]. Intensity information of NFL has been used effectively for the analysis of the NFL [45]. The derivative of the intensity was taken to measure the thickness of NFLDs. The NFLDs were analyzed by Yugesan *et al.* [46] using texture based information. It was observed that the analysis of texture for the NFL is useful for the recognition of NFLD. Kolar *et al.* used Markov random field to differentiate the NFL regions for healthy people compared to those with Glaucoma [47]. Muramatsu *et al.* proposed a method based on texture analysis after transforming the fundus image using Gabor filter [48]. After the image transformation, the curvy bands like pattern of NFLDs appear straight. Pertaining to the

center of ONH, group of elliptical lines was used to model the direction of nerve fiber and then images were converted into polar transformation. To enhance the contrast of NFLD, Gabor filters were used as a post process. The transformed image was then classified for NFLD using a neural network.

B. ANALYSIS OF OPTIC NERVE HEAD

The ONH deformation is another symptom of Glaucoma. ONH is a point where all optic nerves and blood vessels originate from. In the deformation of the ONH, the optic nerve becomes damaged, the size of cup increases and the neuroretinal rim becomes thinner. This type of ONH deformation is called cupping which occurs in the earlier stages of Glaucoma. In the diagnosis of Glaucoma, the cup to disk ration (CDR) is considered a key visual symptom [49], but is rarely used in clinical settings as it is often difficult to recognize the boundary of OC in a retinal fundus images by the naked eye of a medical practitioner. Computer vision techniques have been shown to calculate the correct CDR value consistently and effectively.

1) DETERMINATION OF CDR ON PLAIN FUNDUS PHOTOGRAPH

Determining the boundary between the OC and the OD and hence measuring the CDR is quite challenging in flat fundus images. This is because the border between OD and OC is not easily visible due to interweaving network of capillaries surrounding the OD. Many techniques have been published to counter this problem. Nayak *et al.* have shown that While the CDR is not readily detectable in an RGB colour (Red-Green-Blue) fundus image, the detection becomes considerably easier when using either the red or the green component of the image [50]. Zhang *et al.* have demonstrated the efficacy of a convex envelope based boundary estimation algorithm, that has been shown to mark the border of the OC with good confidence [51]. It has also been shown that the contours



FIGURE 3. (a) A flat fundus image acquired at 40 degree viewing angle. (b) a stereo image of the same eye acquired at a single 34 mm frame. Images courtesy Ophthalmic Photography: Retinal Photography, Angiography, and Electronic Imaging [54].

of the cups can be defined by finding the blood vessels and detect where they bend at the border of the OC and OD [52]. Hatanaka *et al.* proposed a method in which CDR is computed using values of the individual pixels in the fundus image [53]. In this technique, after the segmentation of OD, vertical profiles were attained from the center of OD, and noise is removed by averaging those profiles followed by second derivative of the profiles to determine the OC and hence CDR. Despite the progress in determining an accurate picture of the CDR, there are still much room for improvement.

2) DETERMINATION OF CDR ON STEREO PHOTOGRAPHS

Stereo fundus photography is used to acquire 3D images of the ONH. Stereo fundus images have been shown to offer certain advantages over plain fundus images when detecting OC and OD. The images are acquired using a pair of special retinal fundus cameras that capture a dual (stereo) perspective of the ONH. This gives a 3D perspective to the fundus image making it easier to compute the CDR. It has been shown that the contours of OD and OC can be detected quite efficiently by computing the cross-correlation and stereo disparity between the two fundus images [55]. In another technique proposed by Xu *et al.* [56], stereo disparity was calculated using cross-correlation and minimum difference of the features. Contour of OD and margin of the OC were positioned on the particular depth from the margin of the OC. Abramoff *et al.* implemented a technique on the stereo images that was based on the classification of pixels, region of OC, background and the neuroretinal rim [42]. In the classification of pixels, features of disparity were used along with the color features. CDR was computed by calculating the pixels in the region of OC and neuroretinal rim [57].

Flat and stereo fundus images can be compared in figure 3

V. COMPUTERIZED TECHNIQUES TO DIAGNOSE GLAUCOMA IN RETINAL IMAGES

This section discusses various approaches that have been used in the visual computing domain to detect glaucoma based on the aforementioned symptoms.

A. DETECTION OF GLAUCOMA THROUGH OPTIC NERVE HEAD

Glaucoma disease exists in the region of ONH due to which extraction of this region from the retinal image plays an important role. Therefore, for the segmentation of this region, automated tools have been designed which are based on machine learning and deep learning. The sequential steps of machine learning based techniques include acquiring of the retinal fundus image from the retinal datasets. Some of these datasets include MESSIDOR, Rim-one, Drishti-GS, ORIGA and RIGA. Second step is pre-processing of the retinal image. In pre-processing, quality of retinal image is improved that helps in the segmentation. In this process, different steps can be performed including localization, noise removal, illumination correction, vessel extraction, and contrast enhancement of the retinal image by applying various techniques. Pre-processing also helps in eliminating the irrelevant information from the retinal image and keeps the specific parameter regarding assessment of the disease measurement which makes it more reliable [58]. The next step is segmentation in which region of interest (ROI) is segmented which includes localization of OD, after that process of feature extraction is performed [59]. It is also observed that OD is attained for the diagnosis of Glaucoma without performing this process (i.e. segmentation) [60]. After segmentation, post-processing is performed for achieving better outcome in terms of evaluating parameters. For the screening of Glaucoma, segmentation of OD and OC plays a significant role and there are many existing approaches that have been employed for this purpose. This paper caters these approaches that are used earlier for the segmentation of OD and OC. The common tactics include thresholding that shows some response for the specific pixels that lie below or above from that intensity level. This shows that these techniques use the notion of surfaces, curves, clusters with alike pixels in specific range of group, active contour and active shape model. Moreover, these techniques depend on the boundaries and shape of the region, component and features (i.e. color and intensity).

B. THRESHOLDING BASED TECHNIQUES

It is common and easy approach for the segmentation. This technique converts the colored or gray scale image into binary image. It divides the pixels of image on the basis of intensity level. The segmented image is achieved by choosing the value of threshold that is assigned to the color which is below or above that particular threshold level. Selection of the threshold value is done manually that is based on the features of image. This thresholding is categorized in three types which are global thresholding, variable thresholding and multiple thresholding.

In [61], for the diagnosis of Glaucoma, Ghafer *et al.* proposed an approach for the segmentation of OD. In preprocessing, from RGB retinal image, green channel is selected and sobel operator is used for improving the image quality after which local thresholding is implemented. Afterward, for the extraction of OD region, circular hough transform (CHT) is employed. To get the maximum intensity for OD, thresholding is implemented on preprocessed retinal image. The drawback of this technique was that it has not been implemented on large scale datasets.

In [62], Fuente-Arriaga *et al.* presented an approach for the segmentation of OC. In this method, reference points are used and Ostu thresholding is performed. For observing the vessels movement in the area of the inferior, superior, temporal and nasal, different masks are used with the centroid of OD. The black top hat transform is used for segmentation of vessels along with Ostu thresholding. Then chessboard metric is implemented in all regions for computing the displacement among the vessels centroid which gives the information about the healthy and unhealthy image. Mila *et al.* proposed a method [63] that is based on multi-level thresholding for the segmentation of OD. The retinal blood vessels were eliminated in the pre-processing step. The retinal blood vessels were enhanced by convolving the image with the linear filter and ROI was achieved by applying the local entropy thresholding. The bi-level thresholding is applied for the segmentation of OD. The valley estimation based on histogram was used for defining the clusters comprised of normalization of histogram binning and probability estimation. After that, to segment the region of OD, multi-level thresholding was implemented that is followed by the post-processing step in which morphological operations were used. In this technique, segmentation of OC was not taken into account that is also essential for the screening of Glaucoma disease. Ayushi *et al.* presented a technique in [64] where CDR as well as rim to disc ratio (RDR) has been computed for the diagnosis of Glaucoma disease. Initially ROI is achieved and because of less influence of vessels in red channel, it is used from RGB retinal image for the segmentation of OD and then Ostu thresholding is implemented. The green channel was used for the segmentation of OC as the boundary of OC is perceptible in this channel. Mean and standard deviation were estimated and histogram was analyzed for the mean intensity level. For the segmentation of OC, thresholding is

applied and by subtracting the OD and OC, the neuroretinal rim is attained. Subsequently, RDR is computed by acquiring the temporal and inferior areas using the mask of all quadrants. For the classification purpose, SVM based classifier is employed. This technique lacks in terms of performance. In [65], Tehmina *et al.* proposed a technique to segment the region of OD and OC. In the pre-processing step, resolution of the retinal image is upgraded by bilinear interpolation and contrast is improved by histogram equalization. For the elimination of the noise from the retinal image, mean and median filter are used. For the segmentation of the OD and OC area, Otsu's thresholding is used. After implementing the convex hull, the exact OD and OC is achieved. Although the technique worked well but its effectiveness decreases as color varies from person to person.

C. LEVEL SET BASED TECHNIQUES

In [66], Wong *et al.* proposed an approach to segment the region of OD. Initially, ROI is extracted using pixels of high intensity from histograms. The ROI was taken as initial contour and variational level set based technique are used to segment the OD. OD was not accurately extracted due to the existence of retinal vessels in the region of OD. Therefore, ellipse fitting was applied. For the segmentation of OC, green channel was selected and level set approach is applied based on thresholding. Finally, ellipse fitting has been implemented to get the OC.

In [67], Wong *et al.* further improved the technique by presenting fusion based methodology, for the estimation of CDR to segment the region of OD. Firstly, ROI was achieved using the information of intensity. From RGB retinal image, red channel is selected and variational level set based technique is implemented in order to segment the OD followed by ellipse fitting. Subsequently, values of CDR were computed which were fed to the classifiers. For the classification of image as healthy or unhealthy, SVM and neural network (NN) based classifier were used. In this technique, SVM performed well in comparison with the NN which minimizes the error rate of CDR.

Zhang *et al.* proposed an algorithm in [51], for the OC segmentation. The level set approach based on thresholding, has been implemented for the segmentation of OC. After the segmentation, ellipse fitting is applied that is based on the least square fitting. The boundary of OC achieved after the implementation of ellipse fitting is optimized by implementation of convex hull. The shortcoming of this technique is that it is not beneficial for large scale implementation.

D. CLUSTERING BASED TECHNIQUES

In [68], Xu Yanwu *et al.* proposed an algorithm that is based on low-rank representation of superpixels to segment the region of OC. Initially, linear iterative clustering was used to divide the pixels of OD. Classification of superpixels is performed as neuroretinal rim or OC on the basis of low-rank labeling and then to improve the computational efficiency,

linear kernel is used. The squared forbenius norm has been employed to save the data from data corruption reconstruction error. In this tactic, N-cut label is used and then for the classification of superpixels, majority voting is performed. Although, this technique minimized the non-overlap ratio, but it does not perform well due to the existence of large blood vessels.

Umarani Balakrisnan *et al.* proposed a method in [69] which is based on clustering to segment the OD and OC. Preprocessing is performed to improve the quality of retinal image and for this purpose, Gaussian mask has been used. The clusters are extracted on the basis of mapping and distances, and then using the location of boundaries and objects for the intensity variation, masking is employed for the segmentation purpose.

In [70], Thakur *et al.* presented a technique to segment the region of OD and OC for the screening of Glaucoma disease. In the preprocessing, green and red channels are used for the OD and OC respectively. Then morphological operation (i.e. closing) is used. The fuzzy c-mean clustering is used to segment the OD and OC. Finally, in order to improve the performance, canny edge detector and CHT is implemented.

Khalid *et al.* proposed an algorithm in [71], for the segmentation of OD and OC that is based on fuzzy clustering. At first, ROI is extracted, and values (i.e. min, max) and mean are estimated in the preprocessing step. In the green channel, contrast is better as compared to other channels. Therefore, green channel is used where morphological operations such as dilation and erosion are used to eliminate the vessels. For the segmentation, fuzzy c mean clustering is implemented based on the sum of square using weighting membership functions. The evaluating parameters including sensitivity, accuracy, specificity and F-score are computed. For the validation, receiver operating characteristics with CDR are used. In this technique, CDR above 0.3 is considered as unhealthy. The drawback of this technique is that it does not perform well in terms of accuracy.

E. ACTIVE CONTOUR/SHAPE MODEL BASED TECHNIQUES

Charastek *et al.* presented an algorithm based on active contour to segment the OD. Initially, to improve the shading, retinal image is normalized and non-uniform illumination is estimated using median filtering. Then, ROI is extracted from the retinal image. With the help of Euclidean distances that were used in the thresholding of pre-processed retinal image, the differences in the geometrical features are estimated for eliminating the retinal blood vessels and the noise from the image. Active shape model is implemented for segmenting the OD followed by CHT for OD extraction. The CTREE, LDA and bagging based classifiers are used for the classification of healthy and unhealthy retinal images.

In [72], Yuji proposed a methodology which implements the information of vessel bends for the detection of OC. The blood vessels are eliminated from the blue channel of retinal image, and then to detect the edges of the OC, zero crossing is applied. Afterward, for the final segmentation of OC,

an active contour based model is employed and subsequently spline interpolation is implemented. The sobel gradient direction and p-tile methodology are used for the detection of retinal vessels. k-curvature is used for the finding of vessel bending. With the help of these detected vessel bends, candidates of the OC edges are updated. To get the final OC, spline interpolation is implemented. For the diagnosis of Glaucoma, CDR and RDR are estimated. The drawback of this technique is that the accuracy of classification is not up to the mark.

Megha *et al.* presented a model in [73], for the detection of OD that is based on geodesic active contour. Using green channel, ROI is obtained having the size of 200×200 pixels followed by the application of median filter. Bottom hat filter is applied for the removal of retinal blood vessels, and Ostu thresholding is used to get the vessels binary image. Intensity values of pixels present in the median mask of the image are replaced by the pixels of the retinal vessels. After that, adaptive thresholding is implemented. Subsequently, for the segmentation of OD, CHT and the geodesic active contour is employed. The shortcoming of this technique is that OD with smaller and larger size is not taken into account.

In [74], Cheng *et al.* proposed sparse density technique that is based on dissimilarity. In this technique, three methods are used which are active contour model, super pixel classification and elliptical hough transform (EHT) used in the sequence. Super-classification based technique outperformed the other two methods. Initially, blood vessels are eliminated using morphological operations and non-uniform illumination is improved by linear mapping. The surface fitting and the sparsity terms are applied for the dissimilarity score that is used in the coding of sparse dissimilarity constraint for the segmentation of OD. Least angle regression (LARS) offered by this technique is applied to address the unconstraint optimization problem. Finally, ratio is calculated between the CDRs (i.e. manual and the reference).

F. COMPONENT BASED TECHNIQUES

In [75], Kavitha *et al.* proposed a component based method to segment the region of OD and OC. In the preprocessing, morphological operations (i.e. dilation and erosion) are used for elimination of blood vessels in the red and green channel of the image. Then ROI is extracted and component set based technique is applied for the segmentation of OD and OC. In this technique, neuroretinal rim is assessed using ISNT rule. At the end, CDR and disc damage likelihood (DDLS) are used for the diagnosis of Glaucoma disease.

In [51], Wong *et al.* presented a fusion based technique to detect the OC for the analysis of Glaucoma. To segment the region of OC, histogram is analyzed based on color intensity of vascular architecture. Ellipse fitting is performed to reshape the boundary of OC and CDR is estimated. Subsequently, classification of healthy and unhealthy segmented images are performed using SVM and NN based classifiers.

In [76], a technique based on vessel curves is presented by Wong *et al.* for the segmentation of OC. ROI is detected from OD, and wavelet transform for the interested patch is

achieved using wavelet analysis in the green retinal channel. In order to strengthen the weak edges, canny edge detector is used. The values of the wavelet are used to combine the feature maps that include the information of the color and the gradient in both channels (i.e. red and green). Moreover, SVM based classifier is used to classify the candidate as vessels and non-vessels. The least square technique is used to get curvature, angular difference of the candidates and the highest curvature. Then, Angular gradient of the static vessel bends is computed. Subsequently, nasal points, inferior and the superior region are detected in order to mark the curves in the temporal region, for the segmentation of OC. Finally, to smooth the boundary of OC, ellipse fitting is performed.

VI. PERFORMANCE METRICS

There are many evaluation parameters that have been used for computing and analyzing the effectiveness of the proposed algorithm. In this section, the evaluation parameters are described as follows.

A. SENSITIVITY

Sensitivity (Se) shows the capability to accurately detect the correct pixels. It can be calculated as

$$SN = TP / (TP + FN) \quad (1)$$

where TP shows the true positive and FN shows the false negative. TP region shows that the region of OD or OC is actually present there, and algorithm detects it correctly. Whereas, FN shows that there is no region of OD or OC but algorithms did not detect it correctly. Higher the sensitivity, better will be the performance of the proposed algorithm.

B. SPECIFICITY

Specificity (Sp) shows the capability to accurately detect the pixels that are not part of the region. It can be calculated as

$$Sp = TN / (TN + FP) \quad (2)$$

where TN shows the true negative and FP shows the false positive. TN region shows that the region of OD or OC does not exist and the system predicts it correctly. FP region shows that the region of OD or OC does not exist and the system did not predict it correctly. The algorithm shows better performance if there will be more value of specificity.

C. ACCURACY

Accuracy (Acc) provides the information that how accurately the groundtruths matches the segmented result. The improved accuracy shows better outcome of the proposed algorithm. It can be computed as

$$Acc = Se + Sp / 2 \quad (3)$$

D. DICE

Dice is a measure that provides the information regarding the similarity between the groundtruths and the segmented

region. It can be computed as

$$dm = \frac{2 \times Area(A \cap B)}{Area(A) + Area(B)} \quad (4)$$

where dm shows the dice metric. A shows the segmented region and B show the groundtruth region. The high value of dice shows the better performance of the proposed algorithm.

E. F-SCORE

It is a degree of accuracy that ranges between 0 and 1. The value that is closer to 1 shows the better performance. It can be estimated as

$$Fscore = \frac{2 |Area_{seg} \cap Area_{gt}|}{|Area_{seg}| + |Area_{gt}|} \quad (5)$$

where $Area_{gt}$ shows the area of groundtruth and the $Area_{seg}$ indicates the segmented area.

F. OVERLAP AREA RATIO

It is ratio that provides the information about the overlapping of the region that how much segmented region overlaps the groundtruth region. Greater value of this ratio shows the better performance. It can be calculated as

$$m_1 = \frac{Area_{seg} \cap Area_{gt}}{Area_{seg} \cup Area_{gt}} \quad (6)$$

where m1 shows the overlap area ratio. $Area_{gt}$ shows the area of groundtruth and $Area_{seg}$ shows the area of the segmented region by the proposed algorithm.

G. NON-OVERLAP AREA RATIO

It is ratio that provides information about the dissimilar area between groundtruth region and the segmented region. Lower value of this ratio shows the better performance. It can be estimated as

$$m_2 = 1 - \left(\frac{Area_{seg} \cap Area_{gt}}{Area_{seg} \cup Area_{gt}} \right) \quad (7)$$

where m2 shows the non-overlap area ratio.

H. CORRELATION COEFFICIENT

It is the degree of strength that shows the linearity in relationship between the values of two variables and its value ranges between 0 and 1. If the value is closer to 1, it shows the better performance of the proposed algorithm. It can be computed as

$$r = \frac{n \sum xy - (\sum x)(\sum y)}{\sqrt{n \sum x^2 - (\sum x)^2} \sqrt{n \sum y^2 - (\sum y)^2}} \quad (8)$$

where r shows the correlation coefficient. The x and y, both are the variables, and n shows the total number of observation.

I. RELATIVE ABSOLUTE AREA DIFFERENCE

It shows the relative variation among two regions i.e. groundtruth and the segmented region. Minimum value of the

relative area difference shows the better performance by the proposed method.

$$\text{rad} = \frac{|VD_{\text{seg}} - VD_{\text{ref}}|}{VD_{\text{ref}}} \quad (9)$$

where rad shows the relative area difference. The VD_{ref} shows the vertical diameter of the reference groundtruth and VD_{seg} shows the vertical diameter of the segmented OD.

J. CDR ACCEPTABILITY

It shows the acceptability difference between the two CDR i.e. CDR that is clinically acquired and the CDR that is computed. The acceptable CDR must be less than 0.2, if it is above, the deviation among CDRs will not be acceptable.

$$CDR_{\text{acc}} = CDR_{\text{clinical}} - CDR_{\text{cal}} \leq 0.2 \quad (10)$$

where CDR_{acc} shows the acceptable CDR. The CDR_{clinical} and the CDR_{cal} are clinical and calculated CDR respectively.

K. ERROR

The error E between segmented and groundtruth area can be computed as

$$E = 1 - \frac{\text{Area}(S \cup G)}{\text{Area}(Seg \cap G)} \quad (11)$$

where S represents the segmented region and G represents the ground truth region.

VII. STATE-OF-THE-ART METHODS

A. UNSUPERVISED METHODS

1) OD SEGMENTATION USING RANDOM WALK Algorithm

On the basis of random walk algorithm, an enhanced version of OD segmentation was proposed by Panda *et al.* [77] where new weight composite function is measured by the integration of Gabor texture energy feature and finding the mean curvature which is the key role of this algorithm. Apart from the contortion in the model, suggested algorithm continues with a local energy problem to be minimum and without the curve to be initialized. Performance of the suggested method is analyzed with MESSIDOR, DRIVE, DRISHTI-GS and DIARETDB1 databases. The method achieves specificity 99.83%/99.80%/99.66%/99.94%, precision 92.57%/95.74%/94.41%/93.60% and sensitivity 91.67%/92.03%/95.52%/91.68%. OD detection cases had problems as well, as when the disease was detected the OD limit used to become extremely smooth or discontinuous.

2) CONTOUR ESTIMATES AND OD HOMOGENIZATION

Naqvi *et al.* [78] came up with a method to resolve these issues based on corresponding contour estimates and OD homogenization. To achieve this for the unregulated OD boundary detections, gradient independent activates the contour also for the approximation of OD boundary, and local Laplacian vascular filters are used. The method achieves specificity of 98.96%/98.00%/98.85% accuracy of 94.86%/91.30%/93.64% and sensitivity of 98.60%/96.72%/
98.51% on MESSIDOR, DRIONS-DB and ONHSD datasets respectively.

3) ILM CONTOUR OPTIMIZATION

To enhance the accuracy for extraction of ILM layers, Khalil *et al.* [65] introduced an unprecedented technique. ILM layer contour is also optimized using a contemporary approach in this technique. Addition to that, RPE level endpoint average values were made base to analyze cup edges as a criterion. The method achieves the specificity of 95.00%, accuracy of 94.00% and sensitivity of 93.00% on the dataset of Armed-Forces-Institute-of-Ophthalmology (AFIO).

4) ADAPTIVE HISTOGRAM EQUALIZATION

A computerized diagnostic system which converts color images to gray using adaptive histogram equalization is presented by Acharya *et al.* [60]. This novel technique follows the filtering banks Schmid (S) MR8, MR4 and Leung-Malik (LM). Textons are the micro structures found in the typical images. To extract features of local configuration pattern (LCP), these textons are utilized. The (LCP) features are considered to be important and are picked up by SFFS method using the statistical t-test. Different kind of classifiers were used for classification of glaucoma and normal classes of images. (GRI) Glaucoma index was also enveloped to make the process robust. This method achieved a high classification accuracies of 95.80%.

5) NON-PARAMETRIC AND OPTICAL GIST DESCRIPTOR

Nonparametric and optical GIST descriptor were used as a technique to detect glaucoma proposed by Raghavendra *et al.* [79]. This method suggests novel segmentation of optical disc which is achieved on the basis of the space covered by Rt (radon transformation). Light levels change gets compensated through MCT (modified census transformation) of images obtained from Rt (radon transformation). The MCT images are forwarded to GIST descriptor to conceive spectrum of energy of spatial envelope. The method achieves the specificity of 95.80%, accuracy of 97.00% and sensitivity of 97.80%.

6) VARIATIONAL MODES DECOMPOSITION

Maheshwari *et al.* [80] automated the diagnosis process. VMD (Variational modes decomposition) was utilized for the decomposition of images. Several different features were obtained through VMD elements, such as Yager entropy, Kapoor entropy, Renyi entropy and fractal dimensions. Classification selection was done through Relief F algorithm. Same features were fed to method classification for least square support vector machines (LS-SVM). The method achieves 95%/19% and 94%/79% as classification accuracies utilizing three-fold and ten-fold CV strategies.

7) MULTIPLE DISC DETECTION AND LOCALIZATION

Texture and statistical features were utilized on the basis of regions found in retinal fundus images where a multiple disc

TABLE 2. Performance measures of unsupervised methods for optic disc and optic cup extraction.

Author	Year	Dataset	Performance measures in %			
			ACCURACY	SENSITIVITY	SPECIFICITY	F1Score
[77]	2018	MESSIDOR	-	91.67	99.83	-
		DRIVE	-	92.03	99.8	-
		DRISHTI-GS	-	95.52	99.66	-
		DIARETDB1	-	91.68	99.94	-
[78]	2019	MESSIDOR,	94.86	98.6	98.96	-
		DRIONS-DB	91.3	96.72	98	-
		ONHSD	93.64	98.51	98.85	-
[78]	2017	Armed-Forces-Institute-of-Ophthalmology (AFIO)	93	94	95	-
[60]	2017	-	95.8	-	-	-
[79]	2018	-	97	97.8	95.8	-
[80]	2017	-	94	79		
[81]	2019	ONHSD,	98.8			
		DRIONS	99.3			
		MESSIDOR	99.3			
[82]	2018	RIM-ONE	99.7	84	99.87	
		HRF	96.9	91.52	98.01	
[83]	2018	-	97.67	98		
[84]	2020	MESSIER	99			
		DRIONS	100			
[85]	2018			94		
[86]	2019	DRISHTI-GS1	98			
[87]	2020	INSPIRE	99.31		99.84	
		CHASE-DB1	99.2		99.43	
		viz.HRF	99.73		99.9	
		DRISHTI-GS1	99.31		99.43	
		MESSIDOR	99.72		99.89	
		DRIVE	99.38		99.52	
		ONHSD	99.64		99.82	
		DRIONS-DB	99.37		99.6	
[88]	2019	CPAG	88.5			
[89]	2019	MESSIDOR				
[90]	2019	DI ARETDB1	97.25			
[91]	2018	-	99.3		96.64	
[92]	2019	MESSIDOR	96	96	96	
[93]	2019	DRISHTI-GS	16			90
		RIM-ONE	15			91
[94]	2017	RIM-ONE	97.58	94.44	99	
			99.89 (OD)			
			99.85(OC)			
[95]	2017	DRISHTI-GS	94.1	92.3	95.6	

detection and localization was done through a method proposed by Rehman *et al.* [81]. Analysis and comparisons were done on four of the classifiers where based on common features the most distinctive features were chosen. The method achieves some remarkable accuracies of 98.80%, 99.30% and 99.30% on ONHSD, DRIONS and MESSIDOR databases respectively.

8) MULTI-LAYER PERCEPTION WITH 12-D VECTOR

A correction of his previous work was presented in Zahoor *et al.* [82] where it only showed robust and fast OD segmentation which is the first step in segmentation pipeline of retinal images. In this corrected article, another phases for glaucoma detection is presented. To emphasize area of OC and the NRR, preparation of segmented OD is made.

Moreover, a 12-D vector with a multi-layer perception was utilized to classify pixel based OC segmentation. The ratio for cup to disc is determined by OC, OD segmentation which also extracts the other contextual features. Ensemble subspace classifier was utilized on the basis of decision tree to distinguish between non-Glaucomatous and Glaucomatous images. The method achieves the specificity, accuracy and sensitivity of 99.87% 99.70% and 84.00% for RIM-ONE dataset and 98.01%, 96.90%, and 91.52% for HRF.

9) ANISOTROPIC COMPLEX DUAL TREE WAVELET TRANSFORMATION

Based on anisotropic complex dual tree wavelet transformational features and cup to disc ratio, Kausu et al [83] came up with a new methodology for identifying glaucoma. Using Otsu thresholding and Fuzzy C-Means, the process of clustering optic disc segmentation was achieved. With the help of multi layered perception model, the proposed technique was able to achieve the sensitivity of 98.00% and the accuracy of 97.67%.

10) OD SEGMENTATION AND LOCALIZATION

In another approach introduced by Khan et al. [84], a comprehensive attention was given to segmentation and OD localization. In the methodology de-hazing phenomena was used to enhance the image and then was cropped to the OD area. Transformation of image was done to HSV and for the detection of OD, V was utilized. Using a Laplace transforming cultivated region, the vessels which were extracted from the Green channel with the help of multi-line detector, were removed. In region, growing and local adaptive thresholds Binarization is always applied. Area and eccentricity, the two regions enabled the detection of true OD region. Ellipse fitting method was used to fill the region. The method achieves the accuracies of 99.00 % and 100% on MESSIER and DRIONS databases respectively.

11) COMBINATION OF TEXTURAL AND STRUCTURAL FEATURES

A new methodology is proposed by Khalil et al. [85] that combined textural and structural features which was a more reliable CAD system. The system is designed to make the decision making process more efficient after a detailed analysis of several conditions of glaucoma. The model is based on HTF (Hybrid texture Feature set) and HSF (Hybrid Structural Feature Set) as the two main modules of the system. This new system is also capable of detecting damaged cup which resulted super seeding the best sensitivity by reaching 94%. Two different channels are used to segment discs and cups, none the less, cup to disc ratio comparison method is used to get better accuracies. When comparing glaucoma, outstanding outcomes were achieved with 100 percent accuracy.

12) AUTOMATED GLAUCOMA DIAGNOSIS AND SCREENING

In a technique proposed by Amed Mvoulana et al. [86], for diagnosis and screening of glaucoma, a fully automated

method was developed. On the ultimate screening, some great outcomes were received. This approach has low computational and maintenance costs and can be applied on Mobile health systems. The methodology was applied on DRISHTI-GS1 dataset. With the help of trained specialists, fifty retinal images were provided. On final glaucoma diagnosis and screening, the method achieves the accuracy of 98%.

13) OD SEGMENTATION USING RED CHANNEL SUPER PIXEL AND CIRCULAR HOUGH PEAK VALUE SECTION

Geeta et al. [87] came up with an advanced approach relating to their previous works for localization and segmentations of retinal fundus images in optic discs. They utilized red channel super pixel and circular hough peak value selection in improved ways for segmentation, while for localization, to detect diseases in fundus images, a method of calculation through pixel density was used. The technique was applied on INSPIRE, CHASE-DB1, viz. HRF, DRISHTI-GS1, MESSIDOR, DRIVE, ONHSD and DRIONS datasets. This technique gave better results when compared to current techniques for localization and segmentations. The proposed method achieves high accuracies of 99.5% for segmentation and 99.93% for localization of optic discs.

14) THRESHOLDING BASED DETECTION COMPUTATION

Carrillo et al. [88] also came up with an automatic glaucoma detection technique. He designed the algorithm in such a way that can do all the computations for the detections. This work was all new and was based on thresholding of the cup for segmentation mainly. Moreover, a novel measure was also introduced which calculates the sizes of the discs and cups to get more accurate results. This multi-tasking of the algorithm of getting the thresholds and the sizes simultaneously actually ended up giving improved results for the segmentation of disc as compared to the techniques available. In collaboration with Center of Prevention and Attention of Glaucoma, Bucaramanga in Colombia, the author was able to achieve the accuracies of 88.50 % for Glaucoma detection.

15) CONTRAST LIMITED ADAPTIVE HISTOGRAM EQUALIZATION AND FILTER INTEGRATION

Contrast enhancement and noise removing was achieved in a work by Sonali et al. [89] for fundus images. CLAHE (contrast limited adaptive histogram equalization) and filters integration techniques were used to enhance the color, moreover, to remove de-noising found in the fundus images. Proposed methodologies efficacy was analyzed through different parameters of performance like CoC (Correlation coefficient, SSIM Structural similarity index, EPI (Edge prevention index) and PSNR (Peak signal to noise ratio). The presented method achieves some better percentages for all of the mentioned performance measures when compared with the state of the art methods by applying on MESSIDOR dataset where 0.12% improvement in CoC, 1.19% improvement in SSIM, 1.28% improvement in EPI and a big improvement of 7.85% in PSNR was achieved.

16) BALLISTIC OPTICAL IMAGING FOR OPTICAL COHERENCE TOMOGRAPHY

A novel methodology of Ballistic optical imaging was introduced for OCT (optical coherence tomography) by Kumar *et al.* [90]. This OCT is observed for evaluating the major constraints for glaucoma detection. Retinal nerve fibre layer thickness, cup area, cup volume, disc area, rim and disc area and CDR (cup to disc ratio) are estimated as constraints, which is a work configured and performed by machine intelligence which ends up giving a scheme by ballistic optical imaging for glaucoma detection. To distinguish glaucoma, a correlation clustering is designed which works on a unique adaptive learning system which enables the support vector machines construction suits well to differentiate glaucoma. With the help of Kernel estimations of the density of likelihood distribution, cluster connotation helps to inspect glaucoma signifying the SVC (support vector cluster) to be analogous. Correspondingly on the tomography images of non-glaucomatous, and glaucomatous retina, the optical coherence is retrained on 300 and 600. Moreover, the proposed technique achieves an accuracy rate of 97.25% on DIARETDB1 dataset.

17) STRUCTURAL AND ELECTROPHYSIOLOGICAL TECHNIQUES TO CHARACTERIZE VISUAL IMPAIRMENT

Using structural, psychophysical and electrophysiological methods in glaucoma spectrum, Raimundo *et al.* [91] introduced a technique to characterize early visual impairment which was tested on a local dataset and the results were compared with bit plane slice and local binary methods. In the start of ocular hypertension a considerable damage was found in koniocellular retinocortical, parvo and magno pathways. To monitor the progression for RFNL, longitudinal analysis utilizing OCT (optical coherence tomography) resulted as the best. The outcomes of applying the method resulted in lower sensitivities as compared with the aforementioned new psychophysical methods where the sensitivities were found to be above 90% and specificity above 80% respectively. As conclusion by the authors using high sensitivity functional tests for a minor degree of redundancy, it can be utilized to exploit visual pathways to get an early detection of glaucoma. The psychophysical methods of bit plane and binary turned out to give better performances with the specificity of 96.64%, the accuracies of 99.30%, and the sensitivities of 98.83%. Keeping in view these performance measures are based on all three RGB channels.

18) FEATURE EXTRACTION USING LOCAL BINARY PATTERN

Feature extraction can be referred as the first step for any segmentation. Khunger at al. [92] utilized LBP system to extract features. Moreover, for the recognition of iris which is the cardinal part of glaucoma diseases detection, Daugh Mans calculation method was utilized. Combining both, an automated system was introduced by the author. This automated system can also be divided as ADHF (Automated Detection

using Histogram Features) and ADSN (automatic detection of Non-structural features). This automated system had the capabilities to anticipate any risks associated or symptoms related to glaucoma after careful inspection of the fundus images. Moreover, this novel technique helped to diagnose the dangers associated with the diseases. Earlier, these diagnosis were done manually by ophthalmologists where there is always a chance of human error anticipating the disease and its harms. The reason this automated system is considered as efficient is the performance measure drawn by this technique. This proposed methodology achieves the specificity of 96.00%, accuracies of 96.00%, and the sensitivities of 96.00% respectively when tested on publicly available dataset of MESSIDOR.

19) LEVEL SET BASED ADAPTIVELY REGULARIZED KERNEL-BASED INTUITIONISTIC FUZZY C MEANS

Utilizing the Image processing methods a detailed analysis can be made for OC (Optic cup) and OD (Optic disc) which can be found in retinal fundus images. The OC can be referred as the irregular depression in the centre of the disc, whereas the OD can be referred as the point where nerve cells approach each other, or more generally, the entrance of optic nerve. In a research by Thakur *et al.* [93], a novel approach is presented for a CAD (computer aided diagnostic) system for glaucoma detection where performances of the system is improved utilizing LARKIFCM (Level Set Based Adaptively Regularized Kernel-Based Intuitionistic Fuzzy C means) approach which diagnosis the presence of glaucoma more accurately. This new approach is used for the segmentation of OC and OD which gives more accurate results in less time when applied on DRISHTI-GS and RIM ONE datasets. The dice similarity obtained for DRISHTI-GS is 0.90 whereas the accuracy is 0.16. Similarly, for RIM ONE the dice similarity is 0.91 whereas the accuracy is 0.15.

20) BIOGRAPHY OPTIMIZATION

Biotherapy based optimization is used in a research work by Sarkar *et al.* [94]. The detection of Glaucoma is the CDR value. If this value is more than normal, it shows glaucoma. Authentic localization of OD (optic disc) and to find the cup inside the disc are the main target of the paper. The proposed technique was applied on publicly available dataset of RIM-ONE which achieves the specificity 99.00%, accuracy 97.58%, sensitivity 94.44%, and for OD and OC accuracy its 0.9989 and 0.9985 respectively.

21) CNN BASED SAMPLING

Based on CNN, Zilly *et al.* [95] introduced a sampling methodology to reduce calculation complexity. Output of the last layers are fed as the input of new. A novel softmax classifier is continuously used on the output of all filters then it is applied on test images. The method achieves the specificity of 95.60%, accuracy of 94.10%, and sensitivity of 92.30% on the dataset of DRISHTI-GS1.

B. SUPERVISED METHODS

1) OPTIC DISC LOCALIZATION

Glaucoma risk prediction is proposed in a research by Zhao *et al.* [96] where (OD) optic disc is localized through an automated system with screenings performed for glaucoma pipeline. This pipeline is further divided into three phases. Firstly, To localize the optic disc (OD), sliding window and morphological analysis methods are utilized. Secondly, a fusion loss function was designed, and a novel U-shaped neural network was used to simultaneously break OC and OD. Thirdly, the hidden features and neuroretinal features were fused including energy, entropy, and statistical moments for clinical measurements as CDR (cup to disc ratio) for combining training classifiers of Glaucoma. On ORIGA datasets, the efficiency of the method was analyzed. This method achieves specificity of 77.90%, an accuracy of 82.80%, AUC of 88.90 %, and a sensitivity of 87.60%.

2) VGG-S AND OVERFEAT IMPLEMENTATION

Two different architectures VGG-S and OverFeat were utilized by Orlando *et al.* [97] for automatic glaucoma detection for developing a CNN model. For the validation of current CNN (Overfeat and VGG-S), pre trained architectures for non-fundus images are implemented. Pre-processing is done first for these new obtained fundus images for quality improvements, then ONH segmentation is applied. This method achieves 76.30% and 71.80% as AUC values.

3) GLOBAL GLAUCOMA DETECTION USING CNN

Global Glaucoma Identification was improved by a methodology introduced by Chai *et al.* [98] where he introduced a framework of two fold CNN. As an input, the segmented optic disc was escalated to CNN model, and entire CNN model was fed with the entire image. Moreover, concatenation was done on the CNN model and a fully connected layer was used for classification. This method achieves 81.69% as classification accuracy on the dataset of Beijing Tongren Hospital China.

4) IMPLEMENTATION OF ADVERSARIAL GENERATIVE NETWORKS

Adversarial generative networks were combined by a technique proposed by Jiang *et al.* [99] where he used GL-Net a DCNN multi label model. In two network structures, the GL-Net contains a one discriminator and one generator. General and high level features in the generator are skipped to encourage the mixing of low level information connections. This reduces the down sampling factor and during sampling, it helps to restore detailed information, finally, reducing major loss of information. This method achieves 90.50% and 97.10% as F1 scores for optic cup and optic disc respectively.

5) PATCH DEPENDENT INPUT SPACE ADVERSARIAL LEARNING

A new frameworks, namely, patch dependent input space Adversarial Learning (pOSAL) was introduced by Wang *et al.* [100] which robustly and jointly integrates OC and OD from a number of data sets for fundus images. In lieu of which smooth and accurate segmentation is generated by the network as OC and OD has some unique morphological characteristics. To make the target field segmentation nearer to source one, unsupervised domain adaption is utilized by the pOSAL architecture which also addresses the domain shift issue. To keep the details of segmentation upto fine grained level, pOSAL architecture works as based on patch.

6) OC AND OD SEGMENTATION USING MNET

MNet architecture was introduced by Fu *et al.* [101] which performs the OC and OD segmentation with the help of multi-label system and remaining in one stage structure. Multi-label loss function, Ushaped convolution network and side output layer are parts of the suggested MNet. A receptive field pyramid is constructed by the multi-scale layer input. To understand the hierarchical representation the convolution network in U shape is used, and for different scales of layers, a local prediction map is created by side output layer which works as early classification. With the help of multi label loss function, ultimate map of segmentation is created. Original image is represented in the polar coordinate system to increase the segmentation performance along with implementation of polar transformation. The method achieves the AUC values of 89.97%, 85.08%, and CDR values of 89.98% and 85.08% on SCES and ORIGA datasets respectively.

7) REGION MORPHOLOGY ESTIMATION FOR OC AND OD

To find the ellipse for optical cup (OC) and optical discs (OD), a deep learning framework was introduced in another work by Wang *et al.* [102]. Calculation of cup to disc ratio (CDR) is generally done by estimating the region morphology of OC and OD, but in this approach, parameters are evaluated directly for an ellipse. Two separate modules are utilized to find ellipse in OC and OD regions separately which emphasize the Od region on OC. This method was tested on REFUGE dataset which was capable to achieve CDR of 0.047.

8) PSEUDO-DEPTH RECONSTRUCTION FOR RETINAL FUNDUS IMAGE EVALUATION

The depth of a single retinal fundus image is evaluated in a methodology using deep learning, proposed by Shankaranarayana *et al.* [103]. Although, the insufficiency of labelled data for monocular depth evaluation remain a cause of distress for the author. This problem is eradicated by pre training deep networks where instead of using the auto de-noisy encoder, a novel method namely pseudo-depth reconstruction is used for pre training. This pseudo-depth

TABLE 3. Performance measures of supervised methods for optic disc and optic cup extraction.

Author	Year	Dataset	Performance measures in %				
			Accuracy	Sensitivity	Specificity	AUC	F1Score
[96]	2019	ORIGA	82.80	87.60	77.90	88.90	-
[97]	2017	DRISHTI-GS1	76.3	-	-	-	-
			71.8	-	-	-	-
[98]	2017	BTHC	81.69	-	-	-	-
[99]	2019	DRISHTI-GS1	-	-	-	-	90.50 (OC)
			-	-	-	-	97.10 (OD)
		RIM-ONE-r3	-	-	-	-	-
		REFUGE	-	-	-	-	-
[101]	2018	SCES	-	-	-	89.97	-
		ORIGA	-	-	-	85.08	-
[102]	2019	REFUGE	-	-	-	-	-
[103]	2019	RI-MONE-r3	-	-	-	93.9	-
		ORIGA	-	-	-	84.04	-
[104]	2019	SCES	-	-	-	90.1	-
		ORIGA	-	-	-	85.4	-
[105]	2019	DRISHTI-GS	-	-	-	-	82.20 (OC)
[106]	2020	-	-	80	-	92	-
[107]	2020	Drishti-GS and RIM	100	-	-	-	-
		MESSIDOR Bin Rushed	99.00(OC)	-	-	-	88.00(OC)
[108]	2017	RIM-ONE v.3	-	-	-	-	82
		DRISHTI-GS	-	-	-	-	85
[101]	2018	SINDI, SCES	84.29 (B)	84.78	83.8	91.83	-
[109]	2018	ORIGA	-	-	-	-	-
[110]	2019	DRISHTI-GS	-	-	-	-	0.93
[111]	2019	DRISHTI-GS	-	-	-	-	99.77 (OC)
		-	-	-	-	-	97.38(OD)
		RIM-ONE	-	-	-	-	84.45(OC)
		-	-	-	-	-	96.10(OD)
[112]	2020	REFUGE	-	-	-	-	-
		-	-	-	-	-	-
		-	-	-	-	-	-
[113]	2020	DRISHTI-GS1	86.84	-	-	91.67	-
		ORIGA	90	-	-	92.06	-
		ACRIMA	99.53	-	-	99.98	-
		RIM-ONE	97.37	-	-	100	-
		REFUGE	95.59	-	-	95.1	-
[114]	2020	maghrabi	100	-	-	-	-
		MESSIDOR	98	-	-	-	-
[115]	2020	ORIGA	77	-	-	84.4	-
		-	-	-	-	90.9	-
[116]	2020	RIM-ONE v3	94.8	-	-	-	-
		DRISHTI-GS	93.7	-	-	-	-
		DRIONS-DB	93.4	-	-	-	-
[117]	2020	DRISHTI-GS, RIM-ONE	99.71(OC)	-	-	95.70(OC)	-
			99.66(OD)	-	-	96.90(OD)	-
		RIM-ONE	99.61(OC)	-	-	90.90(OC)	-
			99.56(OD)	-	-	98.70(OD)	-

reconstruction method works effectively, and for retina depth estimation, it works as a proxy. The suggested segmentation was applied on RIMONEr3 and ORIGA databases which achieved 93.90% and 84.04% as AUC respectively.

9) JOINT RCNN

In their other work for optical cup and optical disc segmentations, a region based CNN which is end to end, is introduced by Jiang *et al.* [104]. This end to end CNN is also referred as joint RCNN. The performance of extraction module is increased through atrous convolution in this work. Cup proposed network (CPN) and disc proposed network (DPN) are the proposals for bounding boxes respectively which are introduced by the joint RCNN. When a useful bounding box is selected and after getting insights of optical disc, the disc module suggests to connect CPN and DPN. After the box selection in the suggested network, this phenomena further spreads on the basis of optical cup detection which is a vertical cup to disc ratio (CDR). These can be obtained on corresponding bounding boxes as sections of inscribed ellipse in actual. SCES and ORIGA datasets were used to analyze this method of Joint RCNN. This method achieves AUC of 90.10% and 85.40% for both the datasets respectively.

10) MODIFIED LOCALLY ACTIVE STATISTICAL

With information of appearance and shape, a model of Modified Locally Active Statistical (MLSACM-AS) also with information of appearance and shape, was introduced by Gao *et al.* [105]. To calculate the efficiency of proposed model, DRISHTI-GS database was utilized which was available publicly. This method achieves 82.20% and 95.00% as F1 scores for optic cup and optic disc respectively.

11) NEURAL FIBRE LAYER DEFECT DETECTION

These NFLD are considered as the conventional glaucoma detection techniques by the ophthalmologists. Chisako *et al.* [106] used a combined methodology to find (NFLD) neural fibre layer defect instead of the locations or pixels. This novel method used box based detection which predicted the possible presence of NFLDs. A combined methodology utilized the loss functions of detection and segmentation networks. A drastic change was found in the sensitivities. This method achieves a slight improvement in AUC by 92.00% and a sensitivity of 80.00%.

12) GENERATIVE ADVERSARIAL NETWORK FOR AUTONOMOUS GLAUCOMA DETECTION

(GAN) Generative Adversarial Network, a method introduced by Tomaz *et al.* [107] is a new system for autonomous detection of glaucoma. Image acquisition is done from the available databases. For segmenting optical discs into retinal images, there are three processes. Firstly, training of conditional GAN is performed. Secondly, hole filling is done and thirdly, enhancements are applied. Finally, features are extracted and validation is applied. After Adjustments and improvements, the method was applied on Drishti-GS and

RIM-One databases. This method is able to deliver an accuracy of 100% with an ROC curve of 1.

13) OC AND OD SEGMENTATION BASED ON REGIONS OF INTEREST

On the basis of ROI (regions of interests), Kim *et al.* [118] came up with an idea for automated methods of segmentation for Optic cup and optic disc. To perform the segmentation, U-Net with FCN (Fully convolutional networks) architectures are used. Segmentations were applied separately for optic cup and optic disc on the RIGA datasets comprising Maghrabi, MESSIDOR and Bin Rushed. These datasets are composed of 750 fundus images which are used to test and train the FCNs. The presented method achieves some amazing performances greater than the available algorithms, with 99.00% accuracy, F-Measure of 0.98% and Jaccard Index of 0.95 for Optic disc whereas for optic cup, it shows 99.00% accuracy, F-Measure of 0.88% and Jaccard Index of 0.80 respectively.

14) OC AND OD SEGMENTATION USING U-NET CNN

Also working on automation, Sevalstopolsky *et al.* [108] brought a modified U-Net convolution neural network technique for the segmentation of OC (optic Cup) and OD (Optic Disc) based on deep learning. With the assistance of deep learning, U-Net and CNN technique had a very simple framework which consumed very less time for implementation and prediction that is much better than state of the art. Suggested methodology was implemented on RIM-ONE v.3 and DRISHTI-GS datasets which brought performance measures of Dice 0.82 and IOU of 0.69 for RIM-ONE v.3, and Dice 0.85 and IOU of 0.75 for DRISHTI-GS respectively.

15) GLAUCOMA DETECTION USING RESNET AND DENET

Working on the contextual performances of OD (optic disc), glaucoma detection was done in a research done by Fu *et al.* [119]. The designed system plays with segmentation guided network, a combination of ResNet (residual network) and DENet (Disc-aware ensemble network). Local optic disc region and the hierarchical context of fundus images are integrated. The model works on four different module streams and levels. First stream is global image consideration, second as segmentation guided network, third as local disc region, and the fourth one as disc polar transformation. The results from all these four streams are fed and fused to get the final screening results. These results obtained from the proposed method out performed when compared with the available best methods. The suggested technique achieves specificity, B-accuracy, AUC and sensitivity of 0.8380, 0.8429, 0.9183 and 0.8478 respectively when applied on SINDI and SCES datasets.

16) INTEGRATION OF SEGMENTATION AND LOCALIZATION

A unique method was introduced by XuSun *et al.* [109] where he integrated segmentation and localization in a single method. Although for OC, OD and the glaucoma detection,

segmentation plays an important role but the methods introduced earlier only focused on low level details and used to ignore high level details. These are the approaches earlier researcher used to focus on representation of pixel level and use to ignore object constraints for retinal fundus image analysis. In specific, simultaneous localization of OC and OD helps in taking account for high level details. When the CDR (cup to disc ratio) was calculated, some really nice performances were obtained while working with ORIGA dataset. The proposed technique achieves Overlapping error E for OC as 0.213 and Overlapping error E for OD as 0.069.

17) GLAUCOMA NETWORK

Convolution Neural Networks (CNNs) are capable of getting information in a hierarchy from an image which empower them to differentiate between a non-glaucomic image pattern and a glaucomic image pattern for diagnosis purposes. Mamta *et al.* [110] came up with an enhanced model of U-Net called as G-Net (glaucoma network). For an automated detection system, utilizing CNNs as a core an architecture of deep learning was developed and more accurate results were achieved when G-Net was used in deep learning. This proposed methodology separated OD and OC segmentation, introducing individual U-Net models for OC and OD which resulted in obtaining better results for DRISHTI-GS dataset. The performance values deduced from the suggested technique are 0.88 for IOC and 0.93 for dice metric.

18) PIXEL WISE CLASSIFICATION USING FCNN AND DENSENET

FCNN Fully convolutional networks in cooperation of DenseNet is utilized in a work by Al-Bander *et al.* [120], where he made pixel wise classifications taking advantage of the U shaped architecture DenseNet has with a FCN. Two axes give CDR which is evaluated through the boundaries predicted for OC and OD. Outcomes of the segmentation comes in High Quality. This method is generalized for four datasets. First two appear to perform well better than state of the art without extensive training, and the other two are used to compare the results. Introduced technique was applied on publicly available five datasets where results contain 0.9985 for OC accuracy and 0.9989 for OD accuracy.

19) OC AND OD SEGMENTATION USING RESNET ENCODING AND U-NET DECODING

Shuang Yu *et al.* [111] developed a vigorous segmentation technique for optic cup and optic disc segmentation utilizing an adjusted U-Net design which joins the generally embraced pre-prepared ResNet-34 model as encoding layers with traditional U-Net decoding layers. The model was prepared on the recently accessible RIGA dataset, and accomplished a normal dice estimation of 97.31% for disc segmentation and 87.61% for cup segmentation on a reverse RIGA dataset for CDR when compared with state of the art. Not going with the retraining and tanning of parameters, proposed methodology delivered some comparable figures with state of the art

when applied on RIM-ONE and DRISHTI-GS. After that, the author did fine tuning on two models which achieved average cup dice value of 99.77% and average disc dice value of 97.38% for DRISHTI-GS testing dataset. Similarly, author achieved average cup dice value of 84.45% and average disc dice value of 96.10% for RIM-ONE database. The main advantage of the model is that it behaves as a hybrid combining pre-trained U-Net and ResNet, which helps to overcome the training from the start. Consequently, it further evades over-fitting and accomplishes vigorous execution.

20) GRAPH CONVOLUTION NETWORK

Tian *et al.* [112] introduced a GCN (graph convolution network) technique to deploy OC (optic cup) and OD (Optic disc) segmentation. Feature map is then generated with the help of convolutional neural network in multiscale. Graph nodes concatenated with feature map are used by GCN as an input for segmentation. Jacc (Jaccard Index) was calculated to be 91.60% for OC and 95.64% for OD, whereas the DSC (dice similarity coefficients) are 95.58% and 97.76% for OC and OD respectively when applied on REFUGE dataset.

21) MULTIPLE DEEP CONVOLUTION NEURAL NETWORK

To mitigate the workload of ophthalmologists, Sreng *et al.* [113] presented a two stage automatic glaucoma system with the help of DeepLabv3+ segmentation which is performed on optic disc region, and MDCNN (multiple deep convolution neural networks) are used instead of the encoders. Pretrained deep convolution neural networks are utilized for three different proposals for the stage of classification. 1) Learning Transfer. 2) Utilizing the SVM (support vector machines) for learning feature descriptor. 3) Building ensemble of methods in (1) and (2). This method has been applied on five different datasets for glaucoma classification. When applied on DRISHTI-GS1 dataset, the accuracy was 86.84% with an AUC of 91.67%, for ORIGA dataset, the accuracy was 90.00% with an AUC of 92.06%, for ACRIMA dataset, the accuracy was 99.53% with an AUC of 99.98%, for RIM-ONE dataset, the accuracy was 97.37% with an AUC of 100% and for REFUGE dataset the accuracy was 95.59% with an AUC of 95.10%.

22) MASK-RCNN

Almubarak *et al.* [114] introduced a technique based on stages of algorithm running. The proposed technique was called as Mask-RCNN. The input image is cropped in the first stage then this is feeded to stage two. To produce a final segmentation, weighted loss is utilized to train the network for second stage. A fine tuning strategy is adopted to enhance the detection of first stage. The output of the first stage is combined with the original image used for training to introduce a new training method by different scales. The method was implemented on maghrabi and MESSIDOR datasets. With the help of fine tuning, the algorithm was able to achieve accuracy of 98.04% which was better than previous accuracy

of 96.7% on MESSDOR, and for maghrabi the results went upto 100% from 93.6%.

23) ASSESSMENT OF STRUCTURAL CHANGES IN ONH

For screening of glaucoma at the ONH (optic nerve head), structural changes are evaluated. This evaluation is generally carried out by image segmentation of OC (optic Cup) and OD (optic Disc), after which a CDR (Cup to disc ratio) is calculated. This method can be proven as time taken and costly. To overcome these problems and making the system more efficient, Li *et al.* [115] suggested a method which only works on assessing the structural changes on ONH but the segmentation and CDR calculation is not required all together in the technique. Given experiment utilizes two fold cross validation. The proposed methodology achieves accuracy of 0.77 and AUC of 0.844 when applied on ORIGA dataset.

24) IMAGE ENHANCEMENTS USING GRABCUT ALGORITHM

Barge *et al.* [116] proposed a new method which is based on visibility of optic disc with classified fundus images as bad or good quality. In the ROI to segment the (OD), optic disc as forefront entity Grab Cut algorithm is used after taking only good quality images and applying image enhancements techniques on them. With the help of contour, diameter of the OD is determined. To calculate the efficiency of the OD segmentation, proposed methodology has been applied on RIM-ONE v3, DRISHTI-GS, DRIONS-DB databases and achieved 94.8%, 93.7% and 93.4% as F scores respectively.

25) CUP DISC ENCODER DECODER NETWORK

CDED-Net, a Cup Disc Encoder Decoder Network was introduced in a work by Munazza *et al.* [117] who introduced dense connections for collective segmentation of OC (Optic Cup) and OD (Optic Disc). When comparing with state of the art, this architecture is designed in such a way that it needs very limited parameters and few epochs for training. Data augmentation was also implemented to enhance the accuracies as the evaluation datasets contained a limited number of training images, taking advantage of which the algorithm produced segmentation results in high quality. Moreover, this technique is robust and rigorous enough to be implemented on different diverse datasets which can diagnose several eye related diseases. The ROC curve was displayed for REFUGE dataset in the work. Furthermore, the proposed methodology was implemented on DRISHTI-GS and RIM-ONE datasets which achieved the accuracies of 99.71% and 99.66% for OC and OD for Drishti-GS dataset, whereas the AUC were found to be 0.957 and 0.969. Similarly for RIM-ONE dataset, the accuracies were 99.61% and 99.56% for OC and OD where the AUC figures were found to be 0.909 and 0.987.

VIII. DISCUSSION AND CONCLUSION

There are many retinal ailments that can be the root cause of blindness. One of the leading and incurable disease which

eventually leads to blindness is “Glaucoma”. It is an optic neuropathy which is asymptotic. It affects the optic nerve and results in visual impairment which is irreversible however medication can slow down its rate of progression. There are many factors that can give rise to this disease include IOP, high blood pressure, migraines, obesity and family history but the most common source is IOP. In retina, this disease ‘Glaucoma’ exists in the region of OD therefore accurate detection and segmentation of OD is vital for diagnosis. OD has two parts i.e., OC and neuroretinal rim and for the screening of this ailment, segmentation of OC is also essential to acquire CDR ratio that shows the existence of Glaucoma. Many techniques have been employed earlier to compute CDR ratio but in medical imaging, the computerized techniques have been proven effective and shows notable outcome that assists in correct diagnosis of this ailment.

This research work presents review of computerized techniques for the screening of Glaucoma disease. This paper is divided into six sections. Section 1 provides the detailed introduction of Glaucoma disease. As this disease defaces the optic nerve therefore features of the damaged optic nerve have been discussed include loss of neuroretinal rim, focal notching, asymmetry of OD, PPA, occurrence of changes in blood vessels and hemorrhages in the disc. Earlier different diagnostic approaches are used for screening of Glaucoma which are discussed in this section. This disease has different types and these types are discussed in this section in detail. The potency of computerized techniques is discussed using retinal fundus images. These computerized techniques include detection of NFLD, analysis of ONH, determination of CDR on plain and stereo photographs. In Section 2 different techniques are discussed to detect this disease through ONH. These tactics include thresholding based, level set based, clustering based, active contour/shape model based and component based techniques. In Section 3, datasets of retinal images are given that are used in the detection of this ailment. In section 4, performance metrics have been discussed that helps in computing the parameters. Section 5 presents the state-of-art-techniques based on the supervised and unsupervised methods. In this section 20 techniques based on unsupervised methods and 24 supervised method based approaches have been discussed.

We have discussed state-of-the-art supervised and unsupervised-based learning method. In terms of analytical performance supervised-based learning methods outperformed un-supervised methods. Almost all un-supervised methods require both pre- and post-processing for achieving good results. Some supervised methods also require pre- and post-processing. The models producing superior results had different reasons to achieve such outcomes. Some were structured in a way to “ignore the low level information” and keeping the high level information. For instance, this practice was done in Jiang *et al.* [99] where they utilized GL-Net and DCNN multi label model. Ignoring low level information reduced the down sampling factor, producing F1 scores of 90 and 97 for OC and OD. On the other hand “most

distinctive features” were chosen in a work by Rehman *et al.* [81] to achieve high accuracies of 98.80%, 99.30% and 99.30% on different datasets. “Image Enhancement” after segmentation is also a technique to produce better results. In a work by Tomaz *et al.* [107] hole filling was done after conditional GAN to enhance the image producing 100% accuracy and AUC of 1. “Hybrid Techniques” also play a vital role in producing better performances. Munazza *et al.* [117] performed collective segmentation of OC and OD with the introduction of dense connections. “Data Augmentation” was applied opted by most of the deep learning-based method to produce enough sample for training. “Finding Neural Fibre Layer Defect (NFLD)” is another unique technique with the help of a novel “box based detection method” showed a dramatic increase in sensitivity producing the AUC of 92%. Using state of art methods with a little manipulation also returns better results. Sreng *et al.* [113] utilized DeepLabV3+ for segmentation and MDCNN were used instead of encoders producing AUC of 99.98%. Almubarak *et al.* [114] did “rigorous tuning of images” using such a phenomena produced 100% accuracy. “Using novel techniques for Segmentation and Localization” can also indicate higher performances. Geeta *et al.* [87] implemented segmentation incorporating red channel pixel and circular Hough peak value selection for segmentation and for localization a calculation was done articulated through pixel density.

One thing was common in all of the methods, when it comes to the hardware resource utilization none of them discussed that. Most of the method focused on the performance while ignoring the complexity of the network. Increasing model complication in the pursue of an extra 0.05 in accuracy is something found in most of the networks. Another drawback found in almost all deep learning based networks was the lack of a theoretical framework. This is a frequent issue with deep learning papers on medical image analysis, in general. Both computation complexity and theoretical framework can be two strong area for future research of segmentation in medical images.

REFERENCES

- [1] F. C. Hollows and P. A. Graham, “Intra-ocular pressure, glaucoma, and glaucoma suspects in a defined population,” *Brit. J. Ophthalmol.*, vol. 50, no. 5954089, pp. 570–586, Oct. 1966. [Online]. Available: <https://www.ncbi.nlm.nih.gov/pmc/articles/PMC506274/>
- [2] B. Bengtsson, “The prevalence of glaucoma,” *Brit. J. Ophthalmol.*, vol. 65, no. 1, p. 46, Jan. 1981. [Online]. Available: <http://bjo.bmjjournals.com/content/65/1/46.abstract>
- [3] H. M. Leibowitz, L. R. Krueger, D. E. Maudner, R. C. Milton, M. M. Kini, H. A. Kahn, R. J. Nickerson, J. Pool, T. L. Colton, and J. P. E. A. Ganley, “The Framingham eye study monograph: An ophthalmological and epidemiological study of cataract, glaucoma, diabetic retinopathy, macular degeneration, and visual acuity in a general population of 2631 adults, 1973–1975,” *Surv. Ophthalmol.*, vol. 24, pp. 335–610, Jun. 1980.
- [4] A. Iwase, Y. Suzuki, M. Araie, T. Yamamoto, H. Abe, S. Shirato, Y. Kuwayama, H. K. Mishima, H. Shimizu, G. Tomita, Y. Inoue, and Y. Kitazawa, *The Prevalence Primary Open-Angle Glaucoma Japanese: The Tajimi Study*, vol. 111, no. 9, pp. 1641–1648, Sep. 2004.
- [5] D. J. Spalton, R. A. Hitchings, and P. Hunter, *Atlas of Clinical Ophthalmology With CD-ROM*. Amsterdam, The Netherlands: Elsevier, 2013.
- [6] Z. Zhang, F. S. Yin, J. Liu, W. K. Wong, N. M. Tan, B. H. Lee, J. Cheng, and T. Y. Wong, “ORIGA-light: An online retinal fundus image database for glaucoma analysis and research,” in *Proc. Annu. Int. Conf. IEEE Eng. Med. Biol.*, Aug. 2010, pp. 3065–3068.
- [7] Y. Hagiwara, J. E. W. Koh, J. H. Tan, S. V. Bhandary, A. Laude, E. J. Ciaccio, L. Tong, and U. R. Acharya, “Computer-aided diagnosis of glaucoma using fundus images: A review,” *Comput. Methods Programs Biomed.*, vol. 165, pp. 1–12, Oct. 2018.
- [8] A. Almazroa, S. Alodhayb, E. Osman, E. Ramadan, M. Hummadi, M. Dlaim, M. Alkatee, K. Raahemifar, and V. Lakshminarayanan, “Retinal fundus images for glaucoma analysis: The riga dataset,” *Proc. SPIE*, vol. 10579, Mar. 2018, Art. no. 105790B.
- [9] Y. Hatanaka, A. Noudo, C. Muramatsu, A. Sawada, T. Hara, T. Yamamoto, and H. Fujita, “Automatic measurement of cup to disc ratio based on line profile analysis in retinal images,” in *Proc. Annu. Int. Conf. IEEE Eng. Med. Biol. Soc.*, Aug. 2011, pp. 3387–3390.
- [10] M. S. Haleem, L. Han, J. van Hemert, and B. Li, “Automatic extraction of retinal features from colour retinal images for glaucoma diagnosis: A review,” *Computerized Med. Imag. Graph.*, vol. 37, nos. 7–8, pp. 581–596, Oct. 2013.
- [11] S. S. Kanse and D. M. Yadav, “Retinal fundus image for glaucoma detection: A review and study,” *J. Intell. Syst.*, vol. 28, no. 1, pp. 43–56, Jan. 2019.
- [12] C.-W. Pan, T.-Y. Wong, L. Chang, X.-Y. Lin, R. Lavanya, Y.-F. Zheng, Y.-O. Kok, R.-Y. Wu, T. Aung, and S.-M. Saw, “Ocular biometry in an urban Indian population: The Singapore Indian eye study (SINDI),” *Investigative Ophthalmol. Vis. Sci.*, vol. 52, no. 9, pp. 6636–6642, 2011.
- [13] C. C. Sng, L.-L. Foo, C.-Y. Cheng, J. C. Allen, M. He, G. Krishnaswamy, M. E. Nongpiur, D. S. Friedman, T. Y. Wong, and T. Aung, “Determinants of anterior chamber depth: The Singapore Chinese eye study,” *Ophthalmology*, vol. 119, no. 6, pp. 1143–1150, Jun. 2012.
- [14] A. W. P. Foong, S.-M. Saw, J.-L. Loo, S. Shen, S.-C. Loon, M. Rosman, T. Aung, D. T. H. Tan, E. S. Tai, and T. Y. Wong, “Rationale and methodology for a population-based study of eye diseases in malay people: The singapore malay eye study (SiMES),” *Ophthalmic Epidemiol.*, vol. 14, no. 1, pp. 25–35, Jan. 2007.
- [15] P. Bankhead, C. N. Scholfield, J. G. McGeown, and T. M. Curtis, “Fast retinal vessel detection and measurement using wavelets and edge location refinement,” *PLoS ONE*, vol. 7, no. 3, Mar. 2012, Art. no. e32435.
- [16] J. Sivaswamy, S. R. Krishnadas, G. D. Joshi, M. Jain, and A. U. S. Tabish, “Drishti-GS: Retinal image dataset for optic nerve head(ONH) segmentation,” in *Proc. IEEE 11th Int. Symp. Biomed. Imag. (ISBI)*, Apr. 2014, pp. 53–56.
- [17] F. Fumero, S. Alayón, J. L. Sanchez, J. Sigut, and M. Gonzalez-Hernandez, “RIM-ONE: An open retinal image database for optic nerve evaluation,” in *Proc. 24th Int. Symp. Comput.-Based Med. Syst. (CBMS)*, Jun. 2011, pp. 1–6.
- [18] A. Diaz-Pinto, S. Morales, V. Naranjo, T. Köhler, J. M. Mossi, and A. Navea, “CNNs for automatic glaucoma assessment using fundus images: An extensive validation,” *Biomed. Eng. OnLine*, vol. 18, no. 1, p. 29, Dec. 2019.
- [19] A. Hoover and M. Goldbaum, “Locating the optic nerve in a retinal image using the fuzzy convergence of the blood vessels,” *IEEE Trans. Med. Imag.*, vol. 22, no. 8, pp. 951–958, Aug. 2003.
- [20] M. Ko, C. Leung, and T. Yuen, “Automated segmentation of optic nerve head for the topological assessment,” in *Proc. Global Med. Eng. Phys. Exchanges/Pan Amer. Health Care Exchanges (GMEPE/PAHCE)*, 2016, pp. 1–4.
- [21] J. Staal, M. D. Abràmoff, M. Niemeijer, M. A. Viergever, and B. van Ginneken, “Ridge-based vessel segmentation in color images of the retina,” *IEEE Trans. Med. Imag.*, vol. 23, no. 4, pp. 501–509, Apr. 2004.
- [22] T. Kauppi, V. Kalesnykiene, J.-K. Kamarainen, L. Lensu, I. Sorri, A. Raninen, R. Voutilainen, H. Uusitalo, H. Kälviäinen, and J. Pietilä, “The DIARETDB1 diabetic retinopathy database and evaluation protocol,” in *Proc. Brit. Mach. Vis. Conf.*, vol. 1, 2007, pp. 1–10.
- [23] E. J. Carmona, M. Rincón, J. García-Feijoó, and J. M. Martínez-de-la-Casa, “Identification of the optic nerve head with genetic algorithms,” *Artif. Intell. Med.*, vol. 43, no. 3, pp. 243–259, Jul. 2008, doi: [10.1016/j.artmed.2008.04.005](https://doi.org/10.1016/j.artmed.2008.04.005).

- [24] J. I. Orlando, H. Fu, J. B. Breda, K. van Keer, D. R. Bathula, A. Diaz-Pinto, R. Fang, P. A. Heng, J. Kim, J. Lee, and J. Lee, "Refuge challenge: A unified framework for evaluating automated methods for glaucoma assessment from fundus photographs," *Med. Image Anal.*, vol. 59, Jan. 2020, Art. no. 101570.
- [25] E. Decencière, X. Zhang, G. Cazuguel, B. Lay, B. Cochener, C. Trone, P. Gain, R. Ordonez, P. Massin, A. Erginay, B. Charton, J.-C. Klein, "Feedback on a publicly distributed image database: The messidor database," *Image Anal. Stereol.*, vol. 33, no. 3, pp. 231–234, 2014.
- [26] J. Odstrcilik, R. Kolar, A. Budai, J. Hornegger, J. Jan, J. Gazarek, T. Kubena, P. Černosek, O. Svoboda, and E. Angelopoulou, "Retinal vessel segmentation by improved matched filtering: Evaluation on a new high-resolution fundus image database," *IET Image Process.*, vol. 7, no. 4, pp. 373–383, Jun. 2013.
- [27] M. Armaly, "Genetic determination of cup/disc ratio of the optic nerve," *Arch Ophthalmol.*, vol. 78, no. 1, pp. 35–43, 1967.
- [28] M. E. Yablonski, T. J. Zimmerman, M. A. Kass, and B. Becker, "Prognostic significance of optic disk cupping in ocular hypertensive patients," *Amer. J. Ophthalmol.*, vol. 89, no. 4, pp. 585–592, Apr. 1980.
- [29] M. T. Nicolela and J. R. Vianna, "Optic nerve: Clinical examination," in *Pearls of Glaucoma Management*. Berlin, Germany: Springer, 2016, pp. 17–26.
- [30] A. Almazroa, R. Burman, K. Raahemifar, and V. Lakshminarayanan, "Optic disc and optic cup segmentation methodologies for glaucoma image detection: A survey," *J. Ophthalmol.*, vol. 2015, pp. 1–28, Nov. 2015.
- [31] R. E. Kirsch and D. R. Anderson, "Clinical recognition of glaucomatous cupping," *Amer. J. Ophthalmol.*, vol. 75, no. 3, pp. 442–454, Mar. 1973.
- [32] I. Cher and L. Robinson, "'Thinning' of the neural rim of the optic nerve-head. an altered state, providing a new ophthalmoscopic sign associated with characteristics of glaucoma," *Trans. Ophthalmol. Soc. U.K.*, vol. 93, pp. 213–242, 1973.
- [33] P. J. Airaksinen and A. Heijl, "Visual field and retinal nerve fibre layer in early glaucoma after optic disc haemorrhage," *Acta Ophthalmologica*, vol. 61, no. 2, pp. 186–194, May 2009.
- [34] P. Airaksinen, E. Mustonen, and H. Alanko, "Optic disc hemorrhages. Analysis of stereophotographs and clinical data of 112 patients," *Arch Ophthalmol.*, vol. 99, no. 10, p. 1795, Oct. 1981.
- [35] D. L. C. Diehl, "Prevalence and significance of optic disc hemorrhage in a longitudinal study of glaucoma," *Arch. Ophthalmol.*, vol. 108, no. 4, p. 545, Apr. 1990.
- [36] H. Uchida, S. Ugurlu, and J. Caprioli, "Increasing peripapillary atrophy is associated with progressive glaucoma," *Ophthalmology*, vol. 105, no. 8, pp. 1541–1545, Aug. 1998.
- [37] F. E. Fantes and D. R. Anderson, "Clinical histologic correlation of human peripapillary anatomy," *Ophthalmology*, vol. 96, no. 1, pp. 20–25, Jan. 1989.
- [38] J. Jonas and G. Naumann, "Parapapillary chorioretinal atrophy in normal and glaucoma eyes. II. Correlations," *Investigative Ophthalmol. Vis. Sci.*, vol. 30, no. 5, pp. 919–926, 1989.
- [39] J. R. Ehrlich and N. M. Radcliffe, "The role of clinical parapapillary atrophy evaluation in the diagnosis of open angle glaucoma," *Clin. Ophthalmol.*, vol. 4, p. 971, Sep. 2010.
- [40] A. Septiarini, R. Pulungan, A. Harjoko, and R. Ekantini, "Peripapillary atrophy detection in fundus images based on sectors with scan lines approach," in *Proc. 3rd Int. Conf. Informat. Comput. (ICIC)*, Oct. 2018, pp. 1–6.
- [41] K. K. W. Chan, F. Tang, C. C. Y. Tham, A. L. Young, and C. Y. Cheung, "Retinal vasculature in glaucoma: A review," *BMJ Open Ophthalmol.*, vol. 1, no. 1, Jul. 2017, Art. no. e000032.
- [42] M. D. Abràmoff, M. K. Garvin, and M. Sonka, "Retinal imaging and image analysis," *IEEE Rev. Biomed. Eng.*, vol. 3, pp. 169–208, Jan. 2010. [Online]. Available: <http://www.ncbi.nlm.nih.gov/pmc/articles/PMC3131209/>
- [43] R. Thomas, K. Loibl, and R. Parikh, "Evaluation of a glaucoma patient," *Indian J. Ophthalmol.*, vol. 59, no. 7, p. 43, 2011.
- [44] E. Peli, T. R. Hedges, and B. Schwartz, "Computer measurement of retinal nerve fiber layer striations," *Appl. Opt.*, vol. 28, no. 6, pp. 1128–1134, Mar. 1989. [Online]. Available: <http://ao.osa.org/abstract.cfm?URI=ao-28-6-1128>
- [45] S. Y. Lee, K. K. Kim, J. M. Seo, D. M. Kim, H. Chung, K. S. Park, and H. C. Kim, "Automated quantification of retinal nerve fiber layer atrophy in fundus photograph," in *Proc. 26th Annu. Int. Conf. IEEE Eng. Med. Biol. Soc.*, vol. 1, Sep. 2004, pp. 1241–1243.
- [46] R. H. Eikelboom and C. J. Barry, "Texture analysis of retinal images to determine nerve fibre loss," in *Proc. 14th Int. Conf. Pattern Recognit.*, vol. 2, 1998, pp. 1665–1667.
- [47] R. Kolář and P. Vácha, "Texture analysis of the retinal nerve fiber layer in fundus images via Markov random fields," in *Proc. World Congr. Med. Phys. Biomed. Eng.*, O. Dössel and W. C. Schlegel, Eds. Berlin, Germany: Springer, Sep. 2009, pp. 247–250.
- [48] C. Muramatsu, Y. Hayashi, A. Sawada, Y. Hatanaka, T. Hara, T. Yamamoto, and H. Fujita, "Detection of retinal nerve fiber layer defects on retinal fundus images for early diagnosis of glaucoma," *J. Biomed. Opt.*, vol. 15, no. 1, 2010, Art. no. 016021.
- [49] J. Gloster and D. G. Parry, "Use of photographs for measuring cupping in the optic disc," *Brit. J. Ophthalmol.*, vol. 58, no. 10, pp. 850–862, Oct. 1974. [Online]. Available: <http://www.ncbi.nlm.nih.gov/pmc/articles/PMC1215041/>
- [50] J. Nayak, U. R. Acharya, P. S. Bhat, N. Shetty, and T.-C. Lim, "Automated diagnosis of glaucoma using digital fundus images," *J. Med. Syst.*, vol. 33, no. 5, p. 337, Aug. 2008, doi: [10.1007/s10916-008-9195-z](https://doi.org/10.1007/s10916-008-9195-z).
- [51] Z. Zhang, J. Liu, N. S. Cherian, Y. Sun, J. H. Lim, W. K. Wong, N. M. Tan, S. Lu, H. Li, and T. Y. Wong, "Convex hull based neuro-retinal optic cup ellipse optimization in glaucoma diagnosis," in *Proc. Annu. Int. Conf. IEEE Eng. Med. Biol. Soc.*, Sep. 2009, pp. 1441–1444.
- [52] W. W. K. Damon, J. Liu, T. N. Meng, and Y. Fengshou, "Enhancement of optic cup detection through an improved vessel kink detection framework," *Proc. SPIE*, vol. 7624, Mar. 2010, Art. no. 762439.
- [53] Y. Hatanaka, A. Noudo, C. Muramatsu, and H. Fujita, "Vertical cup-to-disc ratio measurement for diagnosis of glaucoma on fundus images," *Proc. SPIE*, vol. 7624, Mar. 2010, Art. no. 76243C.
- [54] P. J. Saine and M. E. Tyler, *Ophthalmic Photography: Retinal Photography, Angiography, and Electronic Imaging*, vol. 132. Boston, MA, USA: Butterworth-Heinemann, 2002.
- [55] E. Corona, S. Mitra, M. Wilson, T. Krile, Y. H. Kwon, and P. Soliz, "Digital stereo image analyzer for generating automated 3-D measures of optic disc deformation in glaucoma," *IEEE Trans. Med. Imag.*, vol. 21, no. 10, pp. 1244–1253, Oct. 2002.
- [56] J. Xu, H. Ishikawa, G. Wollstein, R. A. Bilonick, K. R. Sung, L. Kagemann, K. A. Townsend, and J. S. Schuman, "Automated assessment of the optic nerve head on stereo disc photographs," *Investigative Ophthalmol. Vis. Sci.*, vol. 49, pp. 2512–2517, Mar. 2008. [Online]. Available: <http://www.ncbi.nlm.nih.gov/pmc/articles/PMC2923578/>
- [57] M. D. Abràmoff, W. L. M. Alward, E. C. Greenlee, L. Shuba, C. Y. Kim, J. H. Fingert, and Y. H. Kwon, "Automated segmentation of the optic nerve head from stereo color photographs using physiologically plausible feature detectors," *Investigative Ophthalmol. Vis. Sci.*, vol. 48, pp. 1665–1673, Apr. 2007. [Online]. Available: <http://www.ncbi.nlm.nih.gov/pmc/articles/PMC2739577/>
- [58] L. Kubecka, J. Jan, and R. Kolar, "Retrospective illumination correction of retinal images," *Int. J. Biomed. Imag.*, vol. 2010, Jul. 2010, Art. no. 780262.
- [59] N. Thakur and M. Juneja, "Survey on segmentation and classification approaches of optic cup and optic disc for diagnosis of glaucoma," *Biomed. Signal Process. Control*, vol. 42, pp. 162–189, Apr. 2018.
- [60] U. R. Acharya, S. Bhat, J. E. W. Koh, S. Bhandary, and H. Adeli, "A novel algorithm to detect glaucoma risk using texton and local configuration pattern features extracted from fundus images," *Comput. Biol. Med.*, vol. 88, Jun. 2017.
- [61] R. A. Abdel-Ghafar and T. Morris, "Progress towards automated detection and characterization of the optic disc in glaucoma and diabetic retinopathy," *Med. Informat. Internet Med.*, vol. 32, no. 1, pp. 19–25, Jan. 2007.
- [62] J. A. D. L. Fuente-Arriaga, E. M. Felipe-Riverón, and E. Garduño-Calderón, "Application of vascular bundle displacement in the optic disc for glaucoma detection using fundus images," *Comput. Biol. Med.*, vol. 47, pp. 27–35, Apr. 2014.
- [63] M. Kankanala and S. Kubakaddi, "Automatic segmentation of optic disc using modified multi-level thresholding," in *Proc. IEEE Int. Symp. Signal Process. Inf. Technol. (ISSPIT)*, Dec. 2014, pp. 000125–000130.

- [64] A. Agarwal, S. Gulia, S. Chaudhary, M. K. Dutta, C. M. Travieso, and J. B. Alonso-Hernandez, "A novel approach to detect glaucoma in retinal fundus images using cup-disk and rim-disk ratio," in *Proc. 4th Int. Work Conf. Bioinspired Intell. (IWOBI)*, Jun. 2015, pp. 139–144.
- [65] T. Khalil, M. U. Akram, S. Khalid, and A. Jameel, "Improved automated detection of glaucoma from fundus image using hybrid structural and textural features," *IET Image Process.*, vol. 11, no. 9, pp. 693–700, Sep. 2017.
- [66] D. W. K. Wong, J. Liu, J. H. Lim, X. Jia, F. Yin, H. Li, and T. Y. Wong, "Level-set based automatic cup-to-disc ratio determination using retinal fundus images in ARGALI," in *Proc. 30th Annu. Int. Conf. IEEE Eng. Med. Biol. Soc.*, Aug. 2008, pp. 2266–2269.
- [67] D. W. K. Wong, J. Liu, J. H. Lim, N. M. Tan, Z. Zhang, S. Lu, H. Li, M. H. Teo, K. L. Chan, and T. Y. Wong, "Intelligent fusion of cup-to-disc ratio determination methods for glaucoma detection in ARGALI," in *Proc. Annu. Int. Conf. IEEE Eng. Med. Biol. Soc.*, Sep. 2009, pp. 5777–5780.
- [68] Y. Xu, L. Duan, S. Lin, X. Chen, D. Wong, T. Wong, and J. Liu, "Optic cup segmentation for glaucoma detection using low-rank superpixel representation," in *Proc. MICCA Part*, 2014, pp. 788–795.
- [69] U. Balakrishnan, "NDC-IVM: An automatic segmentation of optic disc and cup region from medical images for glaucoma detection," *J. Innov. Opt. Health Sci.*, vol. 10, no. 3, May 2017, Art. no. 1750007.
- [70] N. Thakur and M. Juneja, "Clustering based approach for segmentation of optic cup and optic disc for detection of glaucoma," *Current Med. Imag. Rev.*, vol. 13, no. 1, pp. 99–105, Jan. 2017.
- [71] N. E. A. Khalid, N. M. Noor, and N. M. Ariff, "Fuzzy c-means (FCM) for optic cup and disc segmentation with morphological operation," *Procedia Comput. Sci.*, vol. 42, pp. 255–262, 2014.
- [72] Y. Hatamaka, Y. Nagahata, C. Muramatsu, S. Okumura, K. Ogohara, A. Sawada, K. Ishida, T. Yamamoto, and H. Fujita, "Improved automated optic cup segmentation based on detection of blood vessel bends in retinal fundus images," in *Proc. 36th Annu. Int. Conf. IEEE Eng. Med. Biol. Soc.*, Aug. 2014, pp. 126–129.
- [73] M. Lotankar, K. Noronha, and J. Koti, "Detection of optic disc and cup from color retinal images for automated diagnosis of glaucoma," in *Proc. IEEE UP Sect. Conf. Electr. Comput. Electron. (UPCON)*, Dec. 2015, pp. 1–6.
- [74] J. Cheng, F. Yin, D. W. K. Wong, D. Tao, and J. Liu, "Sparse dissimilarity-constrained coding for glaucoma screening," *IEEE Trans. Biomed. Eng.*, vol. 62, no. 5, pp. 1395–1403, May 2015.
- [75] S. Kavitha, S. Karthikeyan, and K. Duraiswamy, "Neuroretinal rim quantification in fundus images to detect glaucoma," *Int. J. Comput. Sci. Netw. Secur.*, vol. 10, no. 6, pp. 134–140, 2010.
- [76] W. W. K. Damon, J. Liu, T. N. Meng, Y. Fengshou, and W. T. Yin, "Automatic detection of the optic cup using vessel kinking in digital retinal fundus images," in *Proc. 9th IEEE Int. Symp. Biomed. Imag. (ISBI)*, May 2012, pp. 1647–1650.
- [77] R. Panda, N. B. Puhan, and G. Panda, "Mean curvature and texture constrained composite weighted random walk algorithm for optic disc segmentation towards glaucoma screening," *Healthcare Technol. Lett.*, vol. 5, no. 1, pp. 31–37, Feb. 2018.
- [78] S. S. Naqvi, N. Fatima, T. M. Khan, Z. U. Rehman, and M. A. Khan, "Automatic optic disk detection and segmentation by variational active contour estimation in retinal fundus images," *Signal, Image Video Process.*, vol. 13, no. 6, pp. 1191–1198, Sep. 2019, doi: [10.1007/s11760-019-01463-y](https://doi.org/10.1007/s11760-019-01463-y).
- [79] U. Raghavendra, S. V. Bhandary, A. Gudigar, and U. R. Acharya, "Novel expert system for glaucoma identification using non-parametric spatial envelope energy spectrum with fundus images," *Biocybernetics Biomed. Eng.*, vol. 38, no. 1, pp. 170–180, 2018, doi: [10.1016/j.bbe.2017.11.002](https://doi.org/10.1016/j.bbe.2017.11.002).
- [80] S. Maheshwari, R. B. Pachori, V. Kanhangad, S. V. Bhandary, and U. R. Acharya, "Iterative variational mode decomposition based automated detection of glaucoma using fundus images," *Comput. Biol. Med.*, vol. 88, pp. 142–149, Sep. 2017, doi: [10.1016/j.combiomed.2017.06.017](https://doi.org/10.1016/j.combiomed.2017.06.017).
- [81] Z. U. Rehman, S. S. Naqvi, T. M. Khan, M. Arsalan, M. A. Khan, and M. A. Khalil, "Multi-parametric optic disc segmentation using superpixel based feature classification," *Expert Syst. Appl.*, vol. 120, pp. 461–473, Apr. 2019, doi: [10.1016/j.eswa.2018.12.008](https://doi.org/10.1016/j.eswa.2018.12.008).
- [82] M. N. Zahoor and M. M. Fraz, "A correction to the article fast optic disc segmentation in retina using polar transform," *IEEE Access*, vol. 6, pp. 4845–4849, 2018.
- [83] T. R. Kausu, V. P. Gopi, K. A. Wahid, W. Doma, and S. I. Niwas, "Combination of clinical and multiresolution features for glaucoma detection and its classification using fundus images," *Biocybern. Biomed. Eng.*, vol. 38, no. 2, pp. 329–341, 2018.
- [84] T. M. Khan, M. Mehmood, S. S. Naqvi, and M. F. U. Butt, "A region growing and local adaptive thresholding-based optic disc detection," *PLoS ONE*, vol. 15, no. 1, pp. 1–16, 2020, doi: [10.1371/journal.pone.0227566](https://doi.org/10.1371/journal.pone.0227566).
- [85] T. Khalil, M. U. Akram, H. Raja, A. Jameel, and I. Basit, "Detection of glaucoma using cup to disc ratio from spectral domain optical coherence tomography images," *IEEE Access*, vol. 6, pp. 4560–4576, 2018.
- [86] A. Mvoulana, R. Kachouri, and M. Akil, "Fully automated method for glaucoma screening using robust optic nerve head detection and unsupervised segmentation based cup-to-disc ratio computation in retinal fundus images," *Computerized Med. Imag. Graph.*, vol. 77, Oct. 2019, Art. no. 101643.
- [87] R. G. Ramani and J. J. Shanthamalar, "Improved image processing techniques for optic disc segmentation in retinal fundus images," *Biomed. Signal Process. Control*, vol. 58, Apr. 2020, Art. no. 101832.
- [88] J. Carrillo, L. Bautista, J. Villamizar, J. Rueda, M. Sanchez, and D. Rueda, "Glaucoma detection using fundus images of the eye," in *Proc. STSIVA*, 2019, pp. 1–4.
- [89] S. Sahu, A. K. Singh, S. P. Ghrera, and M. Elhoseny, "An approach for de-noising and contrast enhancement of retinal fundus image using CLAHE," *Opt. Laser Technol.*, vol. 110, pp. 87–98, Feb. 2019. [Online]. Available: <http://www.sciencedirect.com/science/article/pii/S0030399218306637>
- [90] P. J. Kumar, X. Li, T. Binford, Y. Yuan, W. Hu, Y. Yung, M. Pan, and J. Ruby, "Intelligent detection of glaucoma using ballistic optical imaging," *Adv. Eng. Inform.*, vol. 40, pp. 107–129, Mar. 2019.
- [91] M. Raimundo, C. Mateus, P. Faria, B. Oliveira, J. Cardoso, J. F. Silva, J. M. Pereira, and M. Castelo-Branco, "Sensitivity of psychophysical, electrophysiological and structural tests for detection and progression monitoring in ocular hypertension and glaucoma," *Revista Sociedade Portuguesa de Oftalmologia*, vol. 42, no. 1, 2018.
- [92] M. Khunger, T. Choudhury, S. C. Satapathy, and K.-C. Ting, "Automated detection of glaucoma using image processing techniques," in *Emerging Technologies in Data Mining and Information Security*. Singapore: Springer, 2019, pp. 323–335.
- [93] N. Thakur and M. Juneja, "Optic disc and optic cup segmentation from retinal images using hybrid approach," *Expert Syst. Appl.*, vol. 127, pp. 308–322, Aug. 2019.
- [94] D. Sarkar and S. Das, "Automated glaucoma detection of medical image using biogeography based optimization," in *Advances in Optical Science and Engineering*. Singapore: Springer, 2017, pp. 381–388.
- [95] J. Zilly, J. M. Buhmann, and D. Mahapatra, "Glaucoma detection using entropy sampling and ensemble learning for automatic optic cup and disc segmentation," *Computerized Med. Imag. Graph.*, vol. 55, pp. 28–41, Jan. 2017.
- [96] X. Zhao, F. Guo, Y. Mai, J. Tang, X. Duan, B. Zou, and L. Jiang, "Glaucoma screening pipeline based on clinical measurements and hidden features," *IET Image Process.*, vol. 13, no. 12, pp. 2213–2223, Oct. 2019.
- [97] J. I. Orlando, E. Prokofyeva, M. del Fresno, and M. B. Blaschko, "Convolutional neural network transfer for automated glaucoma identification," *Proc. SPIE*, vol. 10160, Jan. 2017, Art. no. 101600U, doi: [10.1117/12.2255740](https://doi.org/10.1117/12.2255740).
- [98] Y. Chai, L. He, Q. Mei, H. Liu, and L. Xu, "Deep learning through two-branch convolutional neuron network for glaucoma diagnosis," in *Proc. Int. Conf. Smart Health*. Hong Kong: Springer, Jun. 2017, pp. 191–201.
- [99] Y. Jiang, L. Duan, J. Cheng, Z. Gu, H. Xia, H. Fu, C. Li, and J. Liu, "JointRCNN: A region-based convolutional neural network for optic disc and cup segmentation," *IEEE Trans. Biomed. Eng.*, vol. 67, no. 2, pp. 335–343, Feb. 2020.
- [100] S. Wang, L. Yu, X. Yang, C.-W. Fu, and P.-A. Heng, "Patch-based output space adversarial learning for joint optic disc and cup segmentation," *IEEE Trans. Med. Imag.*, vol. 38, no. 11, pp. 2485–2495, Nov. 2019.
- [101] H. Fu, J. Cheng, Y. Xu, D. Wing Kee Wong, J. Liu, and X. Cao, "Joint optic disc and cup segmentation based on multi-label deep network and polar transformation," 2018, *arXiv:1801.00926*. [Online]. Available: <http://arxiv.org/abs/1801.00926>

- [102] Z. Wang, N. Dong, S. D. Rosario, M. Xu, P. Xie, and E. P. Xing, "Ellipse detection of optic disc-and-cup boundary in fundus images Zeya Wang, Nanqing Dong, Sean D Rosario, Min Xu, Pengtao Xie, Eric P. Xing," in *Proc. IEEE 16th Int. Symp. Biomed. Imag. (ISBI)*, 2019, pp. 601–604.
- [103] S. M. Shankaranarayana, K. Ram, K. Mitra, and M. Sivaprakasam, "Fully convolutional networks for monocular retinal depth estimation and optic disc-cup segmentation," *IEEE J. Biomed. Health Informat.*, vol. 23, no. 4, pp. 1417–1426, Jul. 2019.
- [104] Y. Jiang, N. Tan, and T. Peng, "Optic disc and cup segmentation based on deep convolutional generative adversarial networks," *IEEE Access*, vol. 7, pp. 64483–64493, May 2019.
- [105] Y. Gao, X. Yu, C. Wu, W. Zhou, X. Wang, and H. Chu, "Accurate and efficient segmentation of optic disc and optic cup in retinal images integrating multi-view information," *IEEE Access*, vol. 7, pp. 148183–148197, 2019.
- [106] C. Muramatsu, "Diagnosis of glaucoma on retinal fundus images using deep learning: Detection of nerve fiber layer defect and optic disc analysis," in *Deep Learning in Medical Image Analysis*. Cham, Switzerland: Springer, 2020, pp. 121–132.
- [107] T. R. V. Bisneto, A. O. de Carvalho Filho, and D. M. V. Magalhães, "Generative adversarial network and texture features applied to automatic glaucoma detection," *Appl. Soft Comput.*, vol. 90, May 2020, Art. no. 106165.
- [108] A. Sevastopolsky, "Optic disc and cup segmentation methods for glaucoma detection with modification of U-net convolutional neural network," *Pattern Recognit. Image Anal.*, vol. 27, no. 3, pp. 618–624, Jul. 2017.
- [109] X. Sun, Y. Xu, M. Tan, H. Fu, W. Zhao, T. You, and J. Liu, "Localizing optic disc and cup for glaucoma screening via deep object detection networks," in *Computational Pathology and Ophthalmic Medical Image Analysis*. Cham, Switzerland: Springer, 2018, pp. 236–244.
- [110] M. Juneja, S. Singh, N. Agarwal, S. Bali, S. Gupta, N. Thakur, and P. Jindal, "Automated detection of glaucoma using deep learning convolution network (G-net)," *Multimedia Tools Appl.*, vol. 79, pp. 15531–15553, Apr. 2019.
- [111] S. Yu, D. Xiao, S. Frost, and Y. Kanagasingam, "Robust optic disc and cup segmentation with deep learning for glaucoma detection," *Computerized Med. Imag. Graph.*, vol. 74, pp. 61–71, Jun. 2019.
- [112] Z. Tian, Y. Zheng, X. Li, S. Du, and X. Xu, "Graph convolutional network based optic disc and cup segmentation on fundus images," *Biomed. Opt. Exp.*, vol. 11, no. 6, pp. 3043–3057, 2020.
- [113] S. Sreng, N. Maneerat, K. Hamamoto, and K. Y. Win, "Deep learning for optic disc segmentation and glaucoma diagnosis on retinal images," *Appl. Sci.*, vol. 10, no. 14, p. 4916, Jul. 2020.
- [114] H. Almubarak, Y. Bazi, and N. Alajlan, "Two-stage mask-RCNN approach for detecting and segmenting the optic nerve head, optic disc, and optic cup in fundus images," *Appl. Sci.*, vol. 10, no. 11, p. 3833, May 2020.
- [115] S. Li, X. Sui, Y. Wang, T. Che, W. Jiao, B. Zhao, and Y. Zheng, "Screening for glaucoma from fundus images via multitask deep learning," *Investigative Ophthalmol. Vis. Sci.*, vol. 61, no. 7, p. 4530, 2020.
- [116] B. Bhatkalkar, A. Joshi, S. Prabhu, and S. Bhandary, "Automated fundus image quality assessment and segmentation of optic disc using convolutional neural networks," *Int. J. Electr. Comput. Eng.*, vol. 10, no. 1, p. 816, Feb. 2020.
- [117] M. Tabassum, T. M. Khan, M. Arsalan, S. S. Naqvi, M. Ahmed, H. A. Madni, and J. Mirza, "CDED-net: Joint segmentation of optic disc and optic cup for glaucoma screening," *IEEE Access*, vol. 8, pp. 102733–102747, 2020.
- [118] J. Kim, S. Kim, H. Chin, H. Kim, N. Kim, and on behalf of the Epidemiologic Survey Committee of the Korean Ophthalmological Society, "Relationships between hearing loss and the prevalences of cataract, glaucoma, diabetic retinopathy, and age-related macular degeneration in Korea," *J. Clin. Med.*, vol. 8, no. 7, p. 1078, Jul. 2019.
- [119] H. Fu, J. Cheng, Y. Xu, C. Zhang, D. W. K. Wong, J. Liu, and X. Cao, "Disc-aware ensemble network for glaucoma screening from fundus image," *IEEE Trans. Med. Imag.*, vol. 37, no. 11, pp. 2493–2501, Nov. 2018.
- [120] B. Al-Bander, B. Williams, W. Al-Nuaimy, M. Al-Taei, H. Pratt, and Y. Zheng, "Dense fully convolutional segmentation of the optic disc and cup in colour fundus for glaucoma diagnosis," *Symmetry*, vol. 10, no. 4, p. 87, Mar. 2018.

FAIZAN ABDULLAH received the master's degree in data analytics from Deakin University, Burwood, VIC, USA. He is currently a Computer Engineer with COMSATS University, Islamabad, personally interested in image processing and artificial intelligence. His two years in Deakin was also mostly based on achieving this goal, starting from information retrieval, to descriptive, statistics, real world, and predictive analytics. He also devoted his time to learn the new methods of research and development in IT, a course to ensure he is up-to date with the new research methodologies. His main focus always remained on how to use any "information" to deduce certain results and observations.

RAKHSHANDA IMTIAZ received the master's degree in computer engineering from the Department of Electrical and Computer Engineering, COMSATS University Islamabad, Islamabad, Pakistan. Her research interests include deep neural networks, computer vision, and pattern recognition.

HUSSAIN AHMAD MADNI received the M.Sc. degree in computer science from the Department of Computer Science, COMSATS University Islamabad (CUI), Islamabad, Pakistan, in 2019. His research interests include deep neural networks, computer vision, and pattern recognition.

HAROON AHMED KHAN (Member, IEEE) received the Ph.D. degree from Lancaster University, U.K. He is currently an Assistant Professor with the Department of Electrical Engineering, COMSATS University, Islamabad, Pakistan. His research interests include machine learning, medical image analysis, scene understanding, and deep learning methods for image analysis.

TARIQ M. KHAN (Member, IEEE) received the Ph.D. degree from Macquarie University, Sydney, NSW, Australia. He is currently working as a Research Fellow with Deakin University. At CUI, he serves as the Head of the Image and Video Processing Research Group (IVPRG). He has over ten years of research and teaching experience in universities, including CUI, Macquarie University, and UET Taxila, Pakistan. He is interested in both digital image processing (with an emphasis on medical imaging) and machine learning. He has published 40 journals and 22 conference papers in well-reputed journals and conferences, such as IEEE TRANSACTIONS ON IMAGE PROCESSING, *Pattern Recognition*, IEEE ACCESS, *Expert Systems with Applications*, *JRTIP*, ICIAR, VCIP, and DICTA. His research has received research funding from Effat University, HEC (Pakistan), MBIE (New Zealand), and KSA International Collaboration Grant over \$1M in past years. His research interests include most aspects of image enhancement, pattern recognition, and image analysis. He was a recipient of several awards, including the iMQRES Scholarship, the Macquarie University Postgraduate Research Student Support (PRSS) travel grants, and SRGP.

MOHAMMAD A. U. KHAN received the B.S. degree from UET Peshawar, Pakistan, in 1992, the M.Sc. degree from the Loughborough University of Technology, U.K., in 1994, and the Ph.D. degree from Georgia Tech, in 1999. Since 1999, he has been actively involved in image processing, pattern recognition, and machine learning. He published extensively in residual vector quantization, directional filter bank, retinal vessel extraction, and signature verification.

SYED SAUD NAQVI (Member, IEEE) received the B.Sc. degree in computer engineering from the COMSATS Institute of Information Technology, Islamabad, Pakistan, in 2005, the M.Sc. degree in electronic engineering from The University of Sheffield, U.K., in 2007, and the Ph.D. degree from the School of Engineering and Computer Science, Victoria University of Wellington, Wellington, New Zealand, in 2016. He is currently working as an Assistant Professor with the COMSATS Institute of Information Technology. His research interests include saliency modeling, medical image analysis, scene understanding, and deep learning methods for image analysis.